Published for SISSA by Springer

Received: June 29, 2022
Revised: October 26, 2022
Accepted: November 5, 2022
Published: November 15, 2022

Near-BPS Skyrmions

Sven Bjarke Gudnason,[a] **Marco Barsanti**[b] **and Stefano Bolognesi**[b]

[a] *Institute of Contemporary Mathematics, School of Mathematics and Statistics, Henan University, Kaifeng, Henan 475004, P. R. China*

[b] *Department of Physics "E. Fermi", University of Pisa and INFN, Sezione di Pisa, Largo Pontecorvo, 3, Ed. C, 56127 Pisa, Italy*

E-mail: gudnason@henu.edu.cn, marco.barsanti@phd.unipi.it, stefanobolo@gmail.com

Abstract: We consider the Skyrme model in the near-BPS limit. The BPS part is made of the sextic term plus a potential and the deformation is made of the standard massive Skyrme model controlled by a small parameter $\epsilon \ll 1$. In order to keep the perturbation under theoretical and computational control, we find a model for which BPS Skyrmions have compact support, henceforth denoted as compactons, and the spherically symmetric $B = 1$ Skyrmion represents the most stable solution. We use the ϵ-expansion scheme to systematically calculate the corrections to the energy and compare with the exact numerical computations in the $B = 1$ sector. Finally, we use the ϵ-expansion scheme to calculate the bound state of two $B = 1$ Skyrmions and its binding energy, which corresponds, prior to quantization, to the deuteron in our model.

Keywords: Solitons Monopoles and Instantons, Effective Field Theories of QCD, Sigma Models

ArXiv ePrint: 2206.09559

https://doi.org/10.1007/JHEP11(2022)092

JHEP11(2022)092

Contents

JHEP11(2022)092

1 Introduction

The Skyrme model [1, 2] is a field-theoretic approach to nuclear physics based on the symmetries of the strong interactions and the topology of chiral symmetry breaking, providing the stability of the baryon as a topological soliton. The topological soliton, also known as the Skyrmion, is exactly the baryon of large-N_c QCD [3, 4]. A similar correspondence between the baryon and the instanton is realized in holographic QCD models, such as the Witten-Sakai-Sugimoto model [5, 6]. In most varieties of the Skyrme model, the binding energies come out too large by roughly an order of magnitude with respect to the

phenomenological ones. This not only has the effect that the ground state energies are imprecise, but also leads to the illusion that the Skyrmions in each topological sector are well separated in field space by an energy barrier, which in turn validates the rigid-body quantization [7] and harmonic vibrational quantization [8, 9] approaches to the quantum problem of nuclei — although this turns out not even to be true for the standard Skyrme model with a massive pion for large baryon numbers [10].

The main approach to lowering binding energies in the Skyrme model is to find a suitable BPS[1] limit of the model, since in such a limit the energy or mass is directly proportional to the topological degree or baryon number, thus yielding vanishing binding energies at the classical level. The idea is then that a suitable small perturbation around the BPS limit would be the right place to look for a phenomenologically viable model. There are several known BPS versions of the Skyrme model: 1) The mode expansion of 5D Yang-Mills theory in flat space as the Skyrme model coupled to an infinite tower of vector mesons — this model is called the Sutcliffe model [24]. 2) The replacement of the standard Skyrme model with a sextic derivative term, which is the topological charge density squared, and a suitable potential — this model is often called the BPS-Skyrme model [25, 26]. 3) The exclusion of the kinetic term and the altercation of the pion mass term from the first to the fourth power — this model is called the lightly-bound Skyrme model [27]. 4) The promotion of the coupling constants to being functions of the isospin conserving part of the chiral Lagrangian field (i.e. the sigma field), which is inspired by the dielectric deformation of Maxwell theory — this model is called the dielectric Skyrme model [28]. 1) The near-BPS limit of the Sutcliffe model is made by truncating the infinite tower of vector mesons; this truncation breaks conformal symmetry and introduces a scale in the model and numerical computations suggest that two or three vector mesons are needed to reach phenomenologically viable binding energies [29, 30]. 2) The near-BPS limit of the BPS-Skyrme model is taken by adding the standard massive Skyrme model to the BPS-Skyrme sector with a suitably small coefficient, which however complicates numerical computations because very large field derivatives are naturally occurring in this limit [31]. A reason of interest in the BPS-Skyrme model is due to the fact that solutions appear as liquid drops of incompressible baryonic matter sharing, therefore, the same features of real nuclei. 3) The near-BPS limit of the lightly-bound Skyrme model is taken by adding the kinetic term and the pion mass term to the model; the resulting Skyrmions become point-particle like [31] and are hence quite different from ordinary Skyrmions with larger symmetries [32]. 4) The near-BPS limit of the dielectric Skyrme model is taken by altering the form of the dielectric coupling constant (function) [28], but the Skyrmions again become point-particle like in the limit where the binding energies become phenomenologically viable [33].

In this paper, we will study the case 2), i.e. that of the BPS-Skyrme model and its near-BPS deformation. For the BPS part, we will take a potential providing no contribution to the pion mass, whereas the perturbation is chosen to be the standard massive Skyrme model — i.e. with the kinetic, the Skyrme and the pion mass terms — all multiplied by a small

[1]Note that the BPS limit studied in this paper is drastically different from the gauge theory BPS limit occurring in supersymmetric field theories, see the discussions in refs. [11–22]; see also the discussion in ref. [23].

JHEP11(2022)092

control parameter, ϵ. This work is a continuation of the ϵ-expansion scheme that we have developed for the case of the baby Skyrme model in the case of compactons (Skyrmions with compact support in the BPS limit) [23] and in the case of baby Skyrmions with exponential (or rather Gaussian) tails [34]. In the baby Skyrme model case, we were able to check the precision and validity of the ϵ-expansion scheme as a perturbative approach to near-BPS solitons by performing very large brute force numerical computations — only possible in the 2-dimensional case. We also found in the previous work, that the precision of the ϵ-expansion scheme is better in the case of compactons as compared to the solitons with tails [34]. Using this result as a guideline, in this paper we search for a viable BPS model with compactons. Due to the BPS solution for compactons having a discontinuous derivative at the compacton boundary, as opposed to the true near-BPS solution, we found in ref. [23] that a certain cusp condition must be imposed at the compacton boundary, making the total field smooth there. This becomes highly nontrivial if the compacton has a complicated shape and we thus limit our search to stable $B = 1$ compactons with spherical symmetry. These criteria limit our model to a rather specific choice, with essentially only one parameter to dial — namely ϵ. Finally, we compute the bound state of two spherically symmetric $B = 1$ compactons by performing PDE solutions within the framework of the semi-analytic ϵ-expansion scheme and compute the binding energy.

The analysis of the near-BPS Skyrme model has been performed in the literature firstly in the series of works [31, 35–37]. Various difficulties emerged from these studies, so that only a partial exploration of the model could be carried out. In refs. [35, 36], a first attempt of an analytic approximation for the near-BPS model has been made using an axially symmetric BPS solution. Then, once inserted into the Lagrangian, a first approximation of the near-BPS energy can be evaluated. Starting from that result and after an appropriate quantization procedure, the binding energies for the various nuclei have been obtained, showing a reasonable agreement with experimental data (mostly for large nuclei). Despite this result, the validity of the entire analysis is questioned in refs. [31, 37]. In fact, as it was proven in the latter references, not all the BPS solutions can be used as first approximation to the near-BPS field. The proper BPS solution must, in fact, respect a mathematical criterion called the restricted harmonic criterion [37]. As that theorem is not respected by the choices made in refs. [35, 36], the entire work must be revisited. Generically, the moduli space — present in the BPS limit — is lifted by a shallow effective potential and as long as the perturbation parameter is sufficiently small, the near-BPS solutions reside close to the BPS solutions in field space. In the case of the BPS-Skyrme model, however, the moduli space is that of volume preserving diffeomorphisms and is infinite dimensional, drastically complicating the problem — both mathematically and numerically. A rigorous mathematical formulation of the variational approach to the problem with volume preserving diffeomorphisms has been studied in ref. [37] and the case of adding the kinetic term to the BPS-Skyrme model is dubbed the restricted harmonic problem. Restricted refers to being in the infinite moduli space of volume preserving diffeomorphisms and harmonic is the minimizer of the kinetic term. In the lack of a better term, we will denote the perturbation by further terms than the kinetic term as generalized restricted harmonic (GRH).

JHEP11(2022)092

Attacking the problem from a different angle, in ref. [31] a full numeric attempt of solving the near-BPS equations of motion has been performed. In that work, exact near-BPS solutions have been found, pushing the parameter ϵ to a small value, around $\epsilon \sim 0.2$. On the contrary, for smaller values of ϵ ($\epsilon < 0.2$), all results are so far numerically inaccessible. In that range, indeed, the numerical solutions developed unwanted spike-like singularities. Such limitation was unfortunate for the study of the binding energy of the system. In fact, a proper estimate yields $\epsilon \sim 0.01$ for fitting the physically small binding energies of nuclei. Again, that analysis is carried out without a full understanding of the near-BPS system — we will comment more on this in the conclusion.

Since the full numerical approach is extremely difficult, in this work we propose a semi-analytical method for exploring the near-BPS Skyrme model, building on the work of refs. [23, 34]. The strategy is based on the expansion of the near-BPS field around a BPS solution, however, with respect to refs. [35, 36], two more steps are considered. Firstly, we face the problem of the restricted harmonic map. Secondly, once that problem is resolved, we explore the system at the next orders of the expansion. As we will see, the results from the next-to-next-to-leading order (N^2LO) are necessary for extracting the binding energy of a multi-Skyrmion configuration. In light of the previous works in the literature, in order to implement our analysis, we have anticipated various technical and methodological difficulties. Moreover, without the possibility to perform numerical checks, it is even more difficult to establish when, and under what circumstances, a given approximation method could fail. To this end, instead of considering immediately the complicated 3D analysis, we previously performed our investigation in the 2D near-BPS baby Skyrme model [23, 34]. For the 2D case, we were able to implement a new semi-analytical method for the near-BPS analysis and, simultaneously, check it with full numerics. The knowledge acquired from those studies serves as a guide in the 3D case studied in this paper.

In light of our previous works, we have chosen the model in such a way to possess the best features of both the previous 2D cases. This means that, for what concerns the BPS sector, we choose a compacton-type BPS model. In this way, we can easily guess the restricted harmonic maps we need for both the cases of a single and multi-Skyrmion configurations. On the other hand, the BPS-deformation is taken to be the original Skyrme model with the pion mass potential. With this choice, a physical pion mass (not depending on ϵ) is included in the system. In this work, we apply the successful techniques developed in refs. [23, 34]. In particular, applying the perturbative scheme to the case of a single near-BPS Skyrmion, we find very good agreement with the exact full-numerical solution. This achievement confirms again the accuracy of our method. Such a result, however, has been obtained only for the topological sector $B = 1$ due to the mathematical difficulties in finding the restricted harmonic solution for $B > 1$.

The paper is organized as follows. In section 2 we set up the model and notation, find the BPS solutions and calculate the generic energy bound. In section 3, we calculate the corrections to the energy of the Skyrmions in the near-BPS limit within the ϵ-expansion scheme to leading order (LO), next-to-leading order (NLO) and next-to-next-to-leading order (N^2LO). The latter two orders utilize a linearized perturbation field. We finally compute the explicit energy corrections to the $B = 1$ spherically symmetric compacton. In

JHEP11(2022)092

section 4, we set up the calculation of the bound state between two spherically symmetric $B = 1$ compactons in the attractive channel and perform the numerical calculations of the perturbation fields, yielding the binding energies of the bound state. In section 5, we convert the physical quantities to physical units. Finally, we conclude with a discussion in section 6.

Details of the calculation of the generic energy bound in section 2 are delegated to appendix A.

2 The model

The model is based on the BPS Skyrme model [25, 26] with small non-BPS deformations with a coefficient $\epsilon \ll 1$. The deformation-part of the Lagrangian is taken, generically, to be the massive [38, 39] Skyrme model [1, 2]. We thus have

$$\begin{aligned}\mathcal{L} &= \mathcal{L}_{\text{BPS}} + \epsilon\mathcal{L}_{\text{deform}} + \mathcal{L}_\lambda \\ &= \Big(c_6\mathcal{L}_6 + \mu^2\mathcal{L}_0\Big) + \epsilon\Big(c_2\mathcal{L}_2 + c_4\mathcal{L}_4 - m_\pi^2 V_{1,1}(U)\Big) + \mathcal{L}_\lambda,\end{aligned} \tag{2.1}$$

with the kinetic (Dirichlet) term, the Skyrme term, sextic term and Lagrange multiplier term[2]

$$\mathcal{L}_2 = \frac{1}{4}\operatorname{tr}(L_\mu L^\mu), \tag{2.2}$$

$$\mathcal{L}_4 = \frac{1}{32}\operatorname{tr}([L_\mu, L_\nu][L^\mu, L^\nu]), \tag{2.3}$$

$$\mathcal{L}_6 = \frac{1}{144}\eta_{\mu\mu'}\epsilon^{\mu\nu\rho\sigma}\epsilon^{\mu'\nu'\rho'\sigma'}\operatorname{tr}(L_\nu L_\rho L_\sigma)\operatorname{tr}(L_{\nu'}L_{\rho'}L_{\sigma'}), \tag{2.4}$$

$$\mathcal{L}_\lambda = \frac{\lambda}{2}(\det U - 1), \tag{2.5}$$

where $L_\mu \equiv U^\dagger\partial_\mu U$ is the left-invariant chiral current and U is the Skyrme field, related to the pions as

$$U = \sigma\mathbf{1}_2 + \mathrm{i}\tau^a\pi^a, \qquad a = 1, 2, 3, \tag{2.6}$$

and the potential $\mathcal{L}_0$, written in the form

$$-\mathcal{L}_0 = V_{s,p}(U) = \frac{1}{sp}\left(1 - \left(\frac{\operatorname{tr} U}{2}\right)^s\right)^p, \tag{2.7}$$

that should not contribute to the pion mass, whereas $V_{1,1}(U) = (1 - \frac{1}{2}\operatorname{tr} U)$ is the standard pion mass term. The metric convention we use in this paper is of the mostly positive signature, the spacetime indices run as $\mu, \nu, \rho, \sigma = 0, 1, 2, 3$, $\eta_{\mu\nu}$ is the flat Minkowski metric and we take $\epsilon^{0123} = 1$. The BPS sector consists of a sixth-order derivative term, which is the topological current squared, as well as a potential term which we take not to

[2]The Lagrange multiplier term vanishes exactly since U is an SU(2) field, but we include it here so that the vector formulation of the Skyrme model restricts the four-vector Φ to the 3-sphere, where $U = \Phi^0\mathbf{1}_2 + \mathrm{i}\tau^a\Phi^a$, $a = 1, 2, 3$.

JHEP11(2022)092

be the pion mass term. The deformation sector, on the other hand, consists of the normal Skyrme model with a pion mass term.

The potentials are consistent with the boundary condition

$$\lim_{|x|\to\infty} U = \mathbf{1}_2, \tag{2.8}$$

which effectively point compactifies 3-space to a 3-sphere: $\mathbb{R}^3 \cup \{\infty\} \simeq S^3$. The nonlinear sigma model constraint $\det U = 1$ makes the target space SU(2) which as a manifold is also a 3-sphere; this is imposed in the model via the Lagrangian multiplier term $\mathcal{L}_\lambda$. A static configuration, $U : S^3 \to S^3$, is thus characterized by the topological charge $B \in \pi_3(S^3) = \mathbb{Z}$, where B is called the baryon number and can be calculated as

$$B = -\frac{1}{24\pi^2} \int \epsilon_{ijk} \operatorname{tr}[L_i L_j L_k] \, \mathrm{d}^3x. \tag{2.9}$$

Using the parametrization

$$U = \cos f \mathbf{1}_2 + \mathrm{i}\tau^a \hat{n}^a \sin f, \qquad \hat{n} = \frac{1}{1+|u|^2}\left(u+\bar{u}, -\mathrm{i}(u-\bar{u}), 1-|u|^2\right), \tag{2.10}$$

with f a real function and u a complex function of spacetime, the Lagrangian components read

$$\mathcal{L}_2 = -\frac{1}{2}\partial_\mu f \partial^\mu f - \frac{2\sin^2 f}{(1+|u|^2)^2}\partial_\mu u \partial^\mu \bar{u}, \tag{2.11}$$

$$\begin{aligned}\mathcal{L}_4 = &-\frac{2\sin^2 f}{(1+|u|^2)^2}\left(\partial_\mu f \partial^\mu f \partial_\nu u \partial^\nu \bar{u} - \partial_\mu f \partial_\nu f \partial^\mu u \partial^\nu \bar{u}\right) \\ &- \frac{2\sin^4 f}{(1+|u|^2)^4}\left((\partial_\mu u \partial^\mu \bar{u})^2 - \partial_\mu u \partial_\nu \bar{u} \partial^\mu u \partial^\nu \bar{u}\right),\end{aligned} \tag{2.12}$$

$$\mathcal{L}_6 = -\frac{4\sin^4 f}{(1+|u|^2)^4}\eta_{\mu\mu'}\epsilon^{\mu\nu\rho\sigma}\epsilon^{\mu'\nu'\rho'\sigma'}\partial_\nu f \partial_\rho u \partial_\sigma \bar{u} \partial_{\nu'} f \partial_{\rho'} u \partial_{\sigma'} \bar{u}. \tag{2.13}$$

The static energy reads

$$\begin{aligned}E &= E_{\mathrm{BPS}} + \epsilon E_{\mathrm{deform}} \\ &= \left(c_6 E_6 - \mu^2 \int_{\mathbb{R}^3} \mathcal{L}_0 \, \mathrm{d}^3x\right) + \epsilon\left(c_2 E_2 + c_4 E_4 + m_\pi^2 \int_{\mathbb{R}^3} V_{1,1} \, \mathrm{d}^3x\right),\end{aligned} \tag{2.14}$$

with the components

$$E_6 = \int_{\mathbb{R}^3} \frac{4\sin^4 f}{(1+|u|^2)^4}\left(\mathrm{i}\epsilon_{ijk}\partial_i f \partial_j u \partial_k \bar{u}\right)^2 \, \mathrm{d}^3x, \tag{2.15}$$

$$E_2 = \int_{\mathbb{R}^3} \left[\frac{1}{2}(\partial_i f)^2 + \frac{2\sin^2 f}{(1+|u|^2)^2}|\partial_i u|^2\right]\mathrm{d}^3x, \tag{2.16}$$

$$\begin{aligned}E_4 = \int_{\mathbb{R}^3} \Bigg[&\frac{2\sin^2 f}{(1+|u|^2)^2}\left((\partial_i f)^2|\partial_j u|^2 - \partial_i f \partial_j f \partial_i u \partial_j \bar{u}\right) \\ &+ \frac{2\sin^4 f}{(1+|u|^2)^4}\left(|\partial_i u|^4 - (\partial_i u \partial_j \bar{u})^2\right)\Bigg]\mathrm{d}^3x.\end{aligned} \tag{2.17}$$

JHEP11(2022)092

In this paper, we consider BPS potential leading to compacton-type solutions of the type

$$-\mathcal{L}_0 = V_{s,p}(U) = \frac{1}{sp}\left(1 - \left(\frac{\operatorname{tr} U}{2}\right)^s\right)^p = \frac{1}{sp}(1-\cos^s f)^p, \tag{2.18}$$

with $(s,p) = (1,2)$, $(2,1)$ and $(2,2)$ (see the next subsection). Obviously, also the pion mass term, given by $(s,p) = (1,1)$, generates a compacton-type soliton but such a potential is already included in the BPS perturbation.

The topological charge in the parametrization (2.10) reads

$$B = -\frac{1}{2\pi^2}\int \frac{2\sin^2 f}{(1+|u|^2)^2}\mathrm{i}\epsilon_{ijk}\partial_i f \partial_j u \partial_k \bar{u}\, \mathrm{d}^3x. \tag{2.19}$$

2.1 BPS solution

Taking the limit $\epsilon = 0$, we can write the static energy as

$$\begin{aligned} E &= \int_{\mathbb{R}^3}\left(\frac{4c_6\sin^4 f}{(1+|u|^2)^4}\left(\mathrm{i}\epsilon_{ijk}\partial_i f\partial_j u\partial_k\bar{u}\right)^2 + \mu^2 V_{s,p}\right)\mathrm{d}^3x \\ &= \int_{\mathbb{R}^3}\left(\sqrt{c_6}\frac{2\sin^2 f}{(1+|u|^2)^2}\mathrm{i}\epsilon_{ijk}\partial_i f\partial_j u\partial_k\bar{u} + \mu\sqrt{V_{s,p}}\right)^2\mathrm{d}^3x \\ &\quad - 4\mu\sqrt{c_6}\int_{\mathbb{R}^3}\frac{\sin^2 f}{(1+|u|^2)^2}\mathrm{i}\epsilon_{ijk}\partial_i f\partial_j u\partial_k\bar{u}\sqrt{V_{s,p}}\,\mathrm{d}^3x, \end{aligned} \tag{2.20}$$

where we have performed a Bogomol'nyi trick in the second equality. The BPS equation is

$$\sqrt{c_6}\frac{2\sin^2 f}{(1+|u|^2)^2}\mathrm{i}\epsilon_{ijk}\partial_i f\partial_j u\partial_k\bar{u} = -\mu\sqrt{V_{s,p}}, \tag{2.21}$$

and the Bogomol'nyi mass is given by the last line of eq. (2.20).

Using the axially symmetric Ansatz for u:

$$u = \tan\left(\frac{\theta}{2}\right)e^{\mathrm{i}N\phi}, \tag{2.22}$$

the BPS equation reads

$$\sin^2(f) f_r = -\frac{\mu\sqrt{V}r^2}{\sqrt{c_6}N}, \tag{2.23}$$

and for the potential $(s,p) = (1,p)$, we have

$$\cos^2\left(\frac{f}{2}\right)\sin^{2-p}\left(\frac{f}{2}\right)f_r = -\frac{2^{\frac{p}{2}-2}\mu r^2}{N\sqrt{pc_6}}. \tag{2.24}$$

Integrating with respect to r yields

$$\begin{aligned} &\frac{2^{2-p}\tan\left(\frac{f}{4}\right)^{1-p}}{(p-4)(p-2)}\left[{}_2F_1\left(\frac{1-p}{2}, 2-p; \frac{3-p}{2}; -\tan^2\left(\frac{f}{4}\right)\right)\right. \\ &\left. + \left(p-4-2(p-2)\cos\left(\frac{f}{2}\right) + (p-2)\cos f\right)\sec^{2p-4}\left(\frac{f}{4}\right)\right] = -\frac{2^{\frac{p}{2}-2}\mu r^3}{3N\sqrt{pc_6}} + \kappa, \end{aligned} \tag{2.25}$$

JHEP11(2022)092

where ${}_2F_1$ is the standard hypergeometric function and κ is an integration constant. If the limit $f \to 0$ of the left-hand side of the above equation diverges, then the soliton has a tail that tends to infinity. If not, the soliton is of compacton type. Taylor expanding the left-hand side yields

$$-\frac{2^{p-2} f^{3-p}}{p-3} + \mathcal{O}(f^{5-p}), \tag{2.26}$$

which reveals that the soliton is indeed a compacton for $p < 3$. The constant κ of the eq. (2.25) must be chosen so as make f respect the boundary conditions

$$f(0) = \pi, \qquad f(R) = 0, \tag{2.27}$$

that guarantee that the soliton bears a nontrivial topological charge (2.19).

For $p = 1$, which corresponds to the standard pion mass term, the left-hand side of (2.25) is invertible

$$\frac{2}{3}\cos^3\left(\frac{f}{2}\right) = \frac{\mu r^3}{6N\sqrt{2c_6}} - \kappa, \tag{2.28}$$

yielding the explicit compacton solution

$$f = 2\arccos\left(\frac{r}{R}\right), \tag{2.29}$$

where we have defined the compacton radius

$$R \equiv \sqrt[3]{\frac{4N\sqrt{2c_6}}{\mu}}, \tag{2.30}$$

and set $\kappa := 0$.

For other values of p (with $s = 1$), the potential does not give an invertible function that enables us to write explicit solutions for f. It will be useful, however, to consider the $p = 2$ solution, for which the BPS solution reduces to

$$f + \sin f = \pi\left(1 - \frac{r^3}{R^3}\right), \tag{2.31}$$

with the compacton radius defined by

$$R \equiv \sqrt[3]{\frac{3\pi\sqrt{2c_6}N}{\mu}}, \tag{2.32}$$

and we have set $\kappa := \frac{\pi}{2}$. The solution is implicit but still simple.

Considering instead the potential $(s, p) = (2, 1)$ in the axially symmetric Ansatz (2.22), the BPS equation reads

$$\sin(f) f_r = -\frac{\mu r^2}{\sqrt{2c_6}N}. \tag{2.33}$$

JHEP11(2022)092

Integrating with respect to r yields

$$f = \arccos\left(\frac{2r^3}{R^3} - 1\right), \tag{2.34}$$

where the compacton radius now is

$$R = \sqrt[3]{\frac{2N\sqrt{2c_6}}{\mu}}, \tag{2.35}$$

where we have set $\kappa := 1$.

Finally, let us consider the potential (2.18) with $(s, p) = (2, 2)$ in the axially symmetric Ansatz (2.22), for which the BPS equation reduces to

$$f_r = -\frac{\mu r^2}{2\sqrt{c_6}N}. \tag{2.36}$$

Integrating with respect to r gives

$$f = \pi\left(1 - \frac{r^3}{R^3}\right), \tag{2.37}$$

where the compacton radius is

$$R = \sqrt[3]{\frac{6\pi\sqrt{c_6}N}{\mu}}, \tag{2.38}$$

and we have set $\kappa := \pi$.

2.2 BPS energy

The Bogomol'nyi mass is given by the total derivative

$$M_{\mathrm{BPS}}^{(s,p)} = -4\mu\sqrt{c_6}\int_{\mathbb{R}^3}\frac{\sin^2 f}{(1+|u|^2)^2}\mathrm{i}\epsilon_{ijk}\partial_i f\partial_j u\partial_k\bar{u}\sqrt{V_{s,p}}\,\mathrm{d}^3x, \tag{2.39}$$

which is the lower bound for the static energy

$$E \geq M_{\mathrm{BPS}}^{(s,p)}. \tag{2.40}$$

Considering the potential (2.18) with $s = 1$ and using the axially symmetric Ansatz (2.22), the Bogomol'nyi mass reads

$$\begin{aligned} M_{\mathrm{BPS}}^{(1,p)} &= -2^{\frac{p}{2}+3}\mu N\sqrt{\frac{c_6}{p}}4\pi\int_0^R \cos^2\left(\frac{f}{2}\right)\sin^{2+p}\left(\frac{f}{2}\right)f_r\,\mathrm{d}r \\ &= 2^{\frac{p}{2}+4}\mu N\sqrt{\frac{c_6}{p}}\pi^{\frac{3}{2}}\frac{\Gamma\left(\frac{3+p}{2}\right)}{\Gamma\left(3+\frac{p}{2}\right)}, \end{aligned} \tag{2.41}$$

where we again have used the boundary conditions

$$f(0) = \pi, \qquad f(R) = 0. \tag{2.42}$$

JHEP11(2022)092

Notice that the Bogomol'nyi mass is proportional to the degree N as it must. For $p = 1, 2$ we have

$$M_{\rm BPS}^{(1,1)} = \frac{128\pi}{15}\sqrt{2c_6}\mu N, \qquad M_{\rm BPS}^{(1,2)} = 2\pi^2\sqrt{2c_6}\mu N. \tag{2.43}$$

Considering instead the potential (2.18) with $s = 2$, $p = 1$ and using the axially symmetric Ansatz (2.22), the Bogomol'nyi mass reads

$$\begin{aligned} M_{\rm BPS}^{(2,1)} &= -\mu N\sqrt{2c_6}4\pi \int_0^R \sin^3(f) f_r \, \mathrm{d}r \\ &= \frac{16\pi}{3}\sqrt{2c_6}\mu N, \end{aligned} \tag{2.44}$$

where we have used the boundary conditions (2.42).

Finally, let us consider the potential (2.18) with $(s, p) = (2, 2)$ with the axially symmetric Ansatz (2.22), for which the Bogomol'nyi mass reads

$$\begin{aligned} M_{\rm BPS}^{(2,2)} &= -\mu\sqrt{c_6}\mu 4\pi \int_0^R \sin^4(f) f_r \, \mathrm{d}r \\ &= \frac{3}{2}\pi^2\sqrt{c_6}\mu N, \end{aligned} \tag{2.45}$$

where we again have used the boundary conditions (2.42).

2.2.1 Energy bound

The general bound for the total energy as a function of $\{\alpha_0, \alpha_2, \alpha_4, \alpha_6\}$ is:

$$\begin{aligned} E \geq 2\pi^2 \Bigg[& 2\mu(\alpha_0\alpha_6 c_6)^{\frac{1}{2}} \langle \widetilde{V}^{\frac{1}{2}} \rangle + 2\sqrt{\mu}(\alpha_4 \epsilon c_4)^{\frac{3}{4}} \big(2(1-\alpha_0)\big)^{\frac{1}{4}} \langle \widetilde{V}^{\frac{1}{4}} \rangle \\ & + 3\epsilon\big((1-\alpha_4)c_4\alpha_2 c_2\big)^{\frac{1}{2}} + 4\big((1-\alpha_6)c_6\big)^{\frac{1}{4}} \left(\frac{1}{2}(1-\alpha_2)\epsilon c_2\right)^{\frac{3}{4}} \Bigg] |B|, \end{aligned} \tag{2.46}$$

where

$$\widetilde{V}(U) = V_{s,p}(U) + \frac{\epsilon m_\pi^2}{\mu^2} V_{1,1}(U), \tag{2.47}$$

is the combined potential of the pion mass term (a perturbation to order ϵ), $V_{s,p}(U)$ is the potential of the BPS sector, B is the topological charge or Skyrmion number and $\langle \cdots \rangle$ is defined as the target-space average of a generic quantity X as

$$\langle X \rangle \equiv -\frac{1}{24\pi^2 B} \int_{\mathbb{R}^3} X \epsilon_{ijk} \, \mathrm{tr}[L_i L_j L_k] \, \mathrm{d}^3x. \tag{2.48}$$

The bound is obtained by numerical optimization with respect to $\alpha_i \in [0, 1]$. For details on the derivation, see appendix A.

As a consistency check, we can set $\mu = c_6 = \alpha_4 = 0$, $\alpha_2 = \epsilon = 1$ and $c_2 = c_4 = 2$, for which we obtain $E \geq 12\pi^2|B|$, which is the standard topological energy bound in Skyrme units [1, 32]. Notice that when $m_\pi > 0$, the integral $\langle \widetilde{V} \rangle$ depends on ϵ, see eq. (A.2).

JHEP11(2022)092

3 Perturbation in ϵ

In this section we consider the ϵ-expansion scheme around the BPS solution. This technique has been developed and tested in the previous works on the baby-Skyrme model [23, 34], where comparison was made with full brute-force numerical computations, hence establishing the accurateness of the framework. Here we adapt it to a more complex model; the idea remains the same but various modifications have to be made. The solution at zeroth order is just the BPS solution. The leading-order correction to the mass is given by the perturbation minimized and evaluated on the BPS solution. This can be done if a certain finiteness condition applies and for the present paper we restrict to this case. The minimization problem of the perturbation is the so-called generalized restricted harmonic problem. We briefly review the conditions and the solutions that are known so far, essentially the $B = 1$ Skyrmion and non-overlapping multi-compactons solutions. We then discuss an approximate criterion, using as a test the axially symmetric solutions, to test if other preferred restricted harmonic solutions could exist. Once we have selected the candidate model for which the $B = 1+1+\dots$ is the most probable restricted harmonic solution, we consider the expansion to higher order in ϵ and the modifications to the leading-order solution.

3.1 Zeroth order

We will now consider perturbing the BPS sector (i.e. the model (2.1) with $\epsilon = 0$) with a small perturbation, $0 < \epsilon \ll 1$. The deformation adds interactions among the Skyrmions leading to bound states with low binding energy (as long as $\epsilon \ll 1$). In this so-called near-BPS limit, the field U can be written as

$$U(x) = U_0(x) + \delta U(\epsilon, x) \qquad \text{with} \qquad \delta U(0, x) = 0, \tag{3.1}$$

where $U_0(x)$ is a BPS solution and δU is a perturbation that depends on ϵ, but not necessarily in an analytic way. Expanding the static energy in ϵ, the zeroth order is simply given by the BPS mass

$$E^{(0)} = M_{\text{BPS}}^{(s,p)}, \tag{3.2}$$

where $M_{\text{BPS}}^{(s,p)}$ is given by eq. (2.39).

3.2 Leading-order correction

The leading-order (LO) correction to the energy, is linear in ϵ and is given by the perturbation part of the Lagrangian, $\mathcal{L}_{\text{deform}}$, evaluated on the background BPS solution

$$\epsilon M_{\text{LO}} = -\epsilon \int_{\mathbb{R}^3} \mathcal{L}_{\text{deform}}(U_0^*)\, \mathrm{d}^3x, \tag{3.3}$$

where U_0^* is the BPS configuration that minimizes the above integral. This solution is required to be *generalized-restricted harmonic* (GRH), using the definition of refs. [34, 37].

Before analyzing this point, it is necessary to check the finiteness of the LO energy contribution. For instance, the compacton solution (2.29) gives a divergent contribution

JHEP11(2022)092

to the LO energy, since the integral (3.3) diverges if $c_2 > 0$. In this paper, in order to consistently implement the perturbative method, we consider only the cases (the potentials) that lead to finite contributions at every order in the expansion. In the following, we provide a criterion for the LO finiteness, valid for BPS solutions of compacton-type.

3.2.1 Finiteness of LO energy

Using as a test the axially symmetric Ansatz (2.22), the LO energy of a compact solution with radius R reads

$$\begin{aligned}\epsilon M_{\rm LO}(N) &= -\epsilon c_2 \int_{\mathbb{R}^3} \mathcal{L}_2 \, \mathrm{d}^3x - \epsilon c_4 \int_{\mathbb{R}^3} \mathcal{L}_4 \, \mathrm{d}^3x + \epsilon m_\pi^2 \int_{\mathbb{R}^3} V_{1,1} \, \mathrm{d}^3x \\ &= 2\pi\epsilon c_2 \int_0^R \left(r^2 f_r^2 + (1+N^2)\sin^2 f \right) \, \mathrm{d}r \\ &\quad + 2\pi\epsilon c_4 \int_0^R \left((1+N^2)\sin^2(f) f_r^2 + \frac{N^2}{r^2}\sin^4 f \right) \, \mathrm{d}r, \\ &\quad + 4\pi\epsilon m_\pi^2 \int_0^R r^2(1-\cos f) \, \mathrm{d}r. \end{aligned} \tag{3.4}$$

For several classes of BPS solutions, we find that the divergence is due to the term $r^2 f_r^2$ that tends to infinity at the border of the compacton (in the limit $r \to R$). We therefore reduce the finite LO energy condition to requesting that

$$\int_{R-\delta}^{R} r^2 f_r^2 \, \mathrm{d}r < \infty, \qquad \text{with} \qquad \delta \ll R. \tag{3.5}$$

Note that in the Lagrangian $\mathcal{L}_4$ the quantity f_r^2 is multiplied by $\sin^2 f$, which alleviates the divergence of the integral since $f \to 0$ for $r \to R$ (see eq. (2.27)). Using the BPS equation (2.23) and the boundary condition (2.27), we can manipulate the condition (3.5) as

$$\int_{R-\delta}^{R} r^2 f_r^2 \, \mathrm{d}r = \int_{\delta'}^{0} r^2(f) \frac{\mathrm{d}f}{\mathrm{d}r} \, \mathrm{d}f = \frac{\mu}{|N|c_6} \int_0^{\delta'} r^4(f) \sqrt{\frac{V_{s,p}}{\sin^4 f}} \, \mathrm{d}f < \infty, \tag{3.6}$$

with $0 < f(R-\delta) = \delta' \ll 1$. Now, it is useful to expand the function $r(f)$ around $f = 0$ as

$$r(f) \simeq R + \left.\frac{\mathrm{d}r(f)}{\mathrm{d}f}\right|_0 f + \frac{1}{2} \left.\frac{\mathrm{d}^2 r(f)}{\mathrm{d}f^2}\right|_0 f^2 + \mathcal{O}(f^3). \tag{3.7}$$

Every positive power of f in this expansion improves the convergence of the integral and thus if we have

$$\frac{\mu R^4}{|N|c_6} \int_0^{\delta'} \sqrt{\frac{V_{s,p}}{\sin^4 f}} \mathrm{d}f < \infty \tag{3.8}$$

then the condition (3.6) consequently holds true. Considering a class of potentials $V_{s,p}$ of the type (2.18), for which $V_{s,p} \simeq f^{2p}$ near $f = 0$, then we have

$$\frac{\mu R^4}{|N|c_6} \int_0^{\delta'} \sqrt{\frac{V_{s,p}}{\sin^4 f}} \, \mathrm{d}f \sim \frac{\mu R^4 s^{p/2}}{2^{p/2}|N|c_6\sqrt{sp}} \int_0^{\delta'} f^{p-2} \, \mathrm{d}f = \frac{\mu R^4 s^{p/2}}{2^{p/2}|N|c_6\sqrt{sp}} \left[\frac{f^{p-1}}{p-1}\right]_0^{\delta'} < \infty. \tag{3.9}$$

JHEP11(2022)092

In order for this condition to hold true, we deduce that p must be greater than 1, i.e. $p > 1$.

Once this criterion is defined, it is an easy check to verify that only the combinations $(s, p) = (1, 2)$ and $(s, p) = (2, 2)$ of the potential (2.18) lead to a finite LO energy. Hence, we will discard the choice $(s, p) = (2, 1)$ that, analogously to the pion-mass potential $(s, p) = (1, 1)$, generates a divergent LO energy for $c_2 > 0$.

3.2.2 Generalized-restricted harmonic

The generalized-restricted harmonic (GRH) solution $U_0^\star$ in eq. (3.3) represents the BPS configuration that extremizes the LO energy within the whole (BPS) moduli space. In particular, to implement the perturbative expansion of the field, we need $U_0^\star$ to be a minimum (at least locally) of the LO energy. In ref. [37], a criterion for the choice of these GRH solutions is discussed for a perturbation of the type $\mathcal{L}_2$ and $\mathcal{L}_2 + \mathcal{L}_4$. The validity of that criterion is not spoiled by the presence of the pion-mass potential $V_{1,1}$, due to the volume-preserving diffeomorphism invariance of the potential energy. In this section, we analyze the GRH problem following different steps. Firstly, we use the theorem developed in ref. [37] to identify the BPS configuration that extremizes (and minimizes) the perturbation energy due to $\mathcal{L}_2$. Then, using again the results of ref. [37], we check if such a configuration is a minimum even for the combination $\mathcal{L}_2 + \mathcal{L}_4$. In the end, we comment on the trivial role of the potential $V_{1,1}$ in this context.

We briefly review the criterion of ref. [37]. Given a smooth map ϕ from the manifold $\mathcal{M}$ to the manifold $\mathcal{N}$, the Dirichlet energy is generally defined as

$$E_2 = \frac{1}{2} \int_{\mathcal{M}} h_{ab}\, g^{ij}\, \partial_i \phi^a \partial_j \phi^b \sqrt{\det g_{kl}}\, \mathrm{d}^d x, \tag{3.10}$$

where $g = g_{ij}\, \mathrm{d}x^i \otimes \mathrm{d}x^j$ and $h = h_{ab}\, \mathrm{d}\phi^a \otimes \mathrm{d}\phi^b$ are the metrics of the manifold $\mathcal{M}$ and $\mathcal{N}$, respectively, and d is the number of (spatial) dimensions (ignoring time here). Using the map ϕ, the pull-back $\phi^* h$ of the metric h to $\mathcal{M}$ is defined as

$$\phi^* h = h_{ab}\, \frac{\partial \phi^a}{\partial x^i} \frac{\partial \phi^b}{\partial x^j}\, \mathrm{d}x^i \otimes \mathrm{d}x^j. \tag{3.11}$$

Among all the maps ϕ with finite Dirichlet energy, connected by volume-preserving diffeomorphisms, a map $\tilde{\phi}$ is restricted harmonic if and only if the one-form

$$\mathrm{div}\, \tilde{\phi}^* h \quad \text{on } \mathcal{M} \text{ is exact.} \tag{3.12}$$

The divergence div of a symmetric $(0, 2)$ tensor $\eta = \eta_{ij}\, \mathrm{d}x^i \otimes \mathrm{d}x^j$ on $\mathcal{M}$ acts as

$$\mathrm{div}\, \eta = D^i \eta_{ij} \mathrm{d}x^j = g^{ik} (\partial_k \eta_{ij} - \Gamma^l_{ki} \eta_{lj} - \Gamma^l_{kj} \eta_{il})\, \mathrm{d}x^j, \tag{3.13}$$

where the connection is $\Gamma^i_{jk} = \frac{1}{2} g^{il} (\partial_k g_{lj} + \partial_j g_{lk} - \partial_l g_{jk})$.

In order to more easily use this criterion, we rewrite the Dirichlet energy for the Skyrmions in the form (3.10). To this end, the field $U \in \mathrm{SU}(2)$ can be decomposed in terms of four scalar fields σ, π^1, π^2 and π^3 as given in eq. (2.6). This relation allows us to define an O(4) vector field Φ^a as

$$\Phi^a = (\sigma, \pi^1, \pi^2, \pi^3) \qquad \text{with} \qquad \Phi^a \Phi^a = 1, \qquad a = 0, 1, 2, 3. \tag{3.14}$$

JHEP11(2022)092

With this notation, the Dirichlet energy E_2 reads

$$E_2 = -\int_{\mathcal{M}} \mathcal{L}_2 \, \mathrm{d}^3x = -\frac{1}{4}\int_{\mathcal{M}} \mathrm{Tr}[L_i L_i] \, \mathrm{d}^3x = \frac{1}{2}\int_{\mathcal{M}} h_{ab}\, g^{ij}\, \partial_i \Phi^a \partial_j \Phi^a \sqrt{\det g_{kl}} \, \mathrm{d}^3x, \quad (3.15)$$

where $h_{ab} = \delta_{ab}$ and $g^{ij} = \delta^{ij}$.

We now apply this theorem to the case of spherically symmetric Skyrmions. In the following, we use spherical coordinates (r, θ, φ) on $\mathcal{M} = \mathbb{R}^3$ and the vector notation Φ^a for the Skyrme field with the constraint $\Phi^a \Phi^a = 1$. Then, we rewrite the spherically symmetric Ansatz (2.22) for a generic $B = N$ compacton in the form

$$\Phi^a = \begin{pmatrix} \cos f(r) \\ \sin f(r) \sin(\theta) \cos(N\varphi) \\ \sin f(r) \sin(\theta) \sin(N\varphi) \\ \sin f(r) \cos(\theta) \end{pmatrix}, \quad (3.16)$$

where the function f depends only on the radial coordinate, r. The metric h is the standard Euclidean metric and the pull-back $\Phi^* h$ of h can be written as

$$\Phi^* h = \frac{\partial \Phi^a}{\partial \tilde{x}^i} \frac{\partial \Phi^a}{\partial \tilde{x}^j} \, \mathrm{d}\tilde{x}^i \otimes \mathrm{d}\tilde{x}^j = f'^2 \mathrm{d}r^2 + \sin^2(f)(\mathrm{d}\theta^2 + N^2 \sin^2(\theta) \, \mathrm{d}\varphi^2), \quad (3.17)$$

with $\mathrm{d}\tilde{x}^i = (\mathrm{d}r, \mathrm{d}\theta, \mathrm{d}\varphi)$.

Taking the divergence of the tensor (3.17), we obtain the one-form

$$\begin{aligned} \mathrm{div}\, \Phi^* h = & \; D^i \left(\partial_i \Phi^a \partial_j \Phi^a\right) \mathrm{d}\tilde{x}^j \\ = & \left(2 f' f'' + \frac{2}{r} f'^2 - (1 + N^2) \frac{\sin^2 f}{r^3}\right) \mathrm{d}r + (1 - N^2) \frac{\sin^2 f}{r^2} \cot\theta \, \mathrm{d}\theta. \end{aligned} \quad (3.18)$$

According to Poincaré's lemma, if the one-form (3.18) is closed then it is exact. Therefore, the solution (3.16) is restricted harmonic if $\mathrm{d}(\mathrm{div}\, \Phi^* h) = 0$, where d is the exterior derivative. Explicitly,

$$\begin{aligned} \mathrm{d}(\mathrm{div}\, \Phi^* h) = & \frac{1}{2}(\partial_i \omega_j - \partial_j \omega_i) \, \mathrm{d}x^i \wedge \mathrm{d}x^j \\ = & (1 - N^2) \frac{\mathrm{d}}{\mathrm{d}r} \left(\frac{\sin^2 f}{r^2}\right) \cot\theta \, \mathrm{d}r \wedge \mathrm{d}\theta. \end{aligned} \quad (3.19)$$

The ratio $\frac{\sin^2 f}{r^2}$ cannot be a constant since that would be incompatible with the boundary conditions (2.27). The only possibility for eq. (3.19) to vanish is therefore $N = \pm 1$. We conclude that a spherically symmetric compacton with arbitrary orientation and topological charge $N = \pm 1$ is a restricted harmonic map. The same proof can be trivially extended to the case of a composition of $B = 1 + 1 + 1 + \cdots$ spherically symmetric compactons placed in $\mathbb{R}^3$ without overlapping one another.

Despite several attempts, we have not been able to analytically find any restricted-harmonic maps different from the spherical $B = N = 1$ BPS configuration. Therefore, in the aim of correctly implementing the perturbative method, in this paper, we will use only that background solution and a multiple non-overlapping composition of it.

JHEP11(2022)092

The use of the spherical $N = 1$ compacton has an important convenience due to a relevant result obtained in ref. [37]. In particular, it has been proved that every hedgehog field is both $\mathcal{L}_2$-restricted harmonic and restricted $\mathcal{L}_4$-critical, and thus restricted $(\mathcal{L}_2+\mathcal{L}_4)$-critical. This result allows us to say that the spherically symmetric $N = 1$ BPS solution is a stationary point of the LO energy E_2+E_4. Moreover, again in ref. [37], such a configuration has been verified to be *stable* restricted $(\mathcal{L}_2+\mathcal{L}_4)$-critical, as we need for our purpose. Once the spherical compacton $B = N = 1$ is identified as a GRH solution, we can easily verify that the presence of the pion-mass potential energy

$$E_\pi = m_\pi^2 \int (1 - \cos f)\sqrt{\det g_{ij}}\, \mathrm{d}^3x, \tag{3.20}$$

does not influence that result. The LO energy E_π is diff-invariant and thus it does not play any role in the choice of the GRH map.

To summarize, both the single spherical $B = 1$ BPS compacton and the composition of non-overlapping $B = 1+1+1+\cdots$ spherical compactons correctly respect the generalized restricted harmonicity criterion and represent local minima of the LO energy. However, being able to consider only this possibility, we will have no indication about the stability or the meta-stability of such a solution within each topological sector. Due to this fact, in the aim of building stable nuclei, we want to focus our analysis only on those near-BPS systems that lead to energetically preferred configurations made by $B = 1 + 1 + 1 + \cdots$ Skyrmions. That information can be extracted from the evaluation of $N_\star$ that is, in the same way of refs. [23, 34], the charge of the spherical configuration that minimizes the energy per nucleon (E/N). The value of $N_\star$ is specific for every type of near-BPS system and thus will help us to choose a suitable potential.

In the next section, we will prove that, if $N_\star > 1$, we certainly know that a GRH map of charge $N > 1$ minimizes the energy per nucleon better than the spherical $N = 1$ solution. Therefore, considering such near-BPS model, a nucleus made of $B = 1+1+1+\cdots$ Skyrmions can be at best meta-stable. On the contrary, if $N_\star \sim 1$ it is possible to have a stable $B = 1 + 1 + 1 + \cdots$ nucleus.

3.2.3 Explicit LO corrections

The leading-order-in-ϵ correction to the energy comes from plugging the BPS solution into the energy functional

$$\begin{aligned}
\epsilon M_{\mathrm{LO}}^{(s,p)}(N) &= -\epsilon c_2 \int_{\mathbb{R}^3} \mathcal{L}_2\, \mathrm{d}^3x - \epsilon c_4 \int_{\mathbb{R}^3} \mathcal{L}_4\, \mathrm{d}^3x + \epsilon m_\pi^2 \int_{\mathbb{R}^3} V_{1,1}\, \mathrm{d}^3x \\
&= 2\pi\epsilon c_2 \int_0^R \left(r^2 f_r^2 + (1+N^2)\sin^2 f\right)\, \mathrm{d}r \\
&\quad + 2\pi\epsilon c_4 \int_0^R \left((1+N^2)\sin^2(f) f_r^2 + \frac{N^2}{r^2}\sin^4 f\right)\, \mathrm{d}r \\
&\quad + 4\pi\epsilon m_\pi^2 \int_0^R r^2(1-\cos f)\, \mathrm{d}r,
\end{aligned} \tag{3.21}$$

where we have used the axially symmetric Ansatz (2.22).

JHEP11(2022)092

Besides the LO energy, analogously to the method of refs. [23, 34], we calculate the value of $N_\star$ in this section, i.e. the charge of the configuration that minimizes the energy per nucleon (E/N). To find such configuration, given the energy of a $B = N$ spherically symmetric BPS solution $U_0^{\rm sph}$

$$E(\epsilon, N) = E_{\rm BPS}(N) + \epsilon M_{\rm LO}(N, U_0^{\rm sph}), \tag{3.22}$$

we must solve

$$\frac{\mathrm{d}}{\mathrm{d}N}\left(\frac{E(\epsilon, N)}{N}\right) = \frac{\mathrm{d}}{\mathrm{d}N}\left(\frac{M_{\rm LO}(N, U_0^{\rm sph})}{N}\right) = 0, \tag{3.23}$$

and find $N_\star$ by solving for N. Note that, in this calculation, the dependence of ϵ vanishes.

Before dealing with the explicit calculation of $N_\star$, we must point out an important difference about the meaning of $N_\star$ between the 2D cases in refs. [23, 34] and here. In refs. [23, 34], once the near-BPS baby Skyrme model is chosen, the value of $N_\star$ identifies which $Q = N$ solution represents the most stable candidate to be the building block of a nucleus (at least at the leading-order approximation). In the baby Skyrme model case, all the axially symmetric solutions of any topological charge are restricted-harmonic and thus, in the calculation of $N_\star$, the LO energies of the different topological sectors are correctly compared. Here, on the contrary, the situation is different. In fact, as shown in the previous section, only the $N = 1$ spherically symmetric compacton is (generalized) restricted harmonic. Thus, for any $N > 1$, the expression (3.22) evaluated on a spherical BPS compacton does not represent the correct LO energy of a $B = N$ near-BPS Skyrmion.

From the above considerations, the calculation of $N_\star$ seems meaningless in the 3D case. The reason for carrying out this calculation is that, with such a result, we can indirectly prove if an unknown GRH configuration (of charge $N > 1$) minimizes E/N better than $N = 1$. We will verify this statement in the following.

Let us consider to have found a spherical BPS solution $U_0^{\rm sph}$ of charge $B = \widetilde{N}$, whose value of the ratio $E/\widetilde{N}$ is smaller than the one calculated for the GRH solution $U_0^{\rm sph}$ of charge $B = 1$, i.e.,

$$\frac{M_{\rm LO}(B = \widetilde{N}, U_0^{\rm sph})}{\widetilde{N}} < \frac{M_{\rm LO}(B = 1, U_0^{\rm sph})}{1}. \tag{3.24}$$

Then, we have

$$\frac{M_{\rm LO}(B = \widetilde{N}, U_0^{\star})}{\widetilde{N}} < \frac{M_{\rm LO}(B = \widetilde{N}, U_0^{\rm sph})}{\widetilde{N}} < \frac{M_{\rm LO}(B = 1, U_0^{\rm sph})}{1}, \tag{3.25}$$

where $U_0^\star$ is the unknown GRH solution of topological charge $B = \widetilde{N}$. In eq. (3.25), we used the fact that a GRH map minimizes the LO energy better than any other BPS maps.

Finding a result of the type (3.24) (that is equivalent of finding $N_\star > 1$), means that surely a GRH solution of charge $B > 1$, more energetically favored than the spherical $B = N = 1$, exists. As a consequence, in that case a near-BPS solution made of $B = 1 + 1 + 1 + \cdots$ Skyrmions would be at best meta-stable.

On the other hand, if we obtain $N_\star \sim 1$, we cannot definitively prove that the configuration $B = 1+1+1+\cdots$ is the one energetically favored, but surely we avoid the previous

JHEP11(2022)092

counter argument. Therefore, in the following we will select the proper constraints to have $N_\star \sim 1$.

We will now calculate the LO energy and the value of $N_\star$ for the different near-BPS systems built with the BPS potential $V_{s,p}$ and $(s,p) = (1,1), (1,2), (2,1), (2,2)$.

For this calculation, it is convenient to have an explicit BPS solution, so we will first consider the case of the potential (2.18) with $s = 1$ and $p = 1$, for which we have the Bogomol'nyi mass (2.43) and BPS solution (2.29). This potential is the pion mass and hence is not a potential that we eventually would want to use, since we want the pion mass to be in the deformation sector. For this exercise, we set $m_\pi := 0$, since $V_{1,1}$ is included instead in the BPS sector. In particular, we get

$$f_r^2 = \frac{4}{R^2 - r^2}, \qquad \sin^2 f = 4\left(1 - \frac{r^2}{R^2}\right)\frac{r^2}{R^2}, \tag{3.26}$$

which means that the leading-order energy does not converge if $c_2 > 0$ is turned on (due to the singularity in the integral over $(rf_r)^2$. Setting $c_2 := 0$, we obtain

$$\epsilon M_{\rm LO}^{(1,1)} = 2\pi\epsilon c_4 \left[(1+N^2)\frac{16}{3R} + N^2\frac{128}{105R}\right], \tag{3.27}$$

where

$$R = \sqrt[3]{N}\tilde{R}, \qquad \tilde{R} = \sqrt[3]{\frac{4\sqrt{2c_6}}{\mu}}. \tag{3.28}$$

The leading-order mass per N has a minimum at

$$N_\star^{(1,1)} = \sqrt{\frac{70}{43}} \simeq 1.276, \tag{3.29}$$

and indeed the $N = 1$ leading-order energy correction per N is smaller than that of the $N = 2$.

Considering instead the potential (2.18) with $s = 2$ and $p = 1$, for which we have the Bogomol'nyi mass (2.44) and BPS solution (2.34), we have

$$f_r^2 = \frac{9r}{R^3 - r^3}, \qquad \sin^2 f = 4\left(1 - \frac{r^3}{R^3}\right)\frac{r^3}{R^3}, \tag{3.30}$$

which again means that the leading-order energy does not converge if $c_2 > 0$ is turned on (due to the singularity in the integral over $(rf_r)^2$). We have again set $m_\pi := 0$ since the BPS solution is massive (as $p = 1$). Setting $c_2 := 0$, we obtain

$$\epsilon M_{\rm LO}^{(2,1)} = 2\pi\epsilon c_4 \left[(1+N^2)\frac{36}{5R} + N^2\frac{36}{55R}\right], \tag{3.31}$$

where

$$R = \sqrt[3]{N}\tilde{R}, \qquad \tilde{R} = \sqrt[3]{\frac{2\sqrt{2c_6}}{\mu}}. \tag{3.32}$$

JHEP11(2022)092

The leading-order mass per N has a minimum at

$$N_\star^{(2,1)} = \sqrt{\frac{11}{6}} \simeq 1.354, \tag{3.33}$$

and indeed the $N = 1$ leading-order energy correction per N is smaller than that of the $N = 2$.

Although the two solutions we have considered now, conveniently have explicit BPS solutions in terms of f, they both yield infinite leading-order corrections to the kinetic term (i.e. $-\int \mathcal{L}_2 \, \mathrm{d}^3x$). Moreover, they have a contribution to the pion mass from the BPS sector, which we want to avoid as we want the pion mass to scale with ϵ in the near-BPS limit. We will therefore consider the case of the potential (2.18) with $(s, p) = (1, 2)$, for which the BPS solution is given by eq. (2.31) and the Bogomol'nyi mass by (2.43). Since the BPS solution (2.31) is not explicit, we have to rewrite the integrals for the leading-order correction to the energy as

$$\begin{aligned} \epsilon M_{\mathrm{LO}}^{(1,2)}(N) = {} & 2\pi\epsilon c_2 \int_\pi^0 \left(r^2 \frac{\partial f}{\partial r} + (1+N^2)\sin^2 f \frac{\partial r}{\partial f} \right) \mathrm{d}f \\ & + 2\pi\epsilon c_4 \int_\pi^0 \left((1+N^2)\sin^2 f \frac{\partial f}{\partial r} + \frac{N^2}{r^2}\sin^4(f) \frac{\partial r}{\partial f} \right) \mathrm{d}f \\ & + \frac{4\pi\epsilon m_\pi^2}{3} \int_\pi^0 (1-\cos f) \frac{\partial r^3}{\partial f} \mathrm{d}f. \end{aligned} \tag{3.34}$$

Using now that

$$r^3 = N\tilde{R}^3 \left(1 - \frac{f + \sin f}{\pi} \right), \tag{3.35}$$

we have

$$\begin{aligned} \frac{\partial r}{\partial f} &= -\frac{\tilde{R} N^{1/3}}{3\pi} \frac{1+\cos f}{\left(1 - \frac{f+\sin f}{\pi}\right)^{\frac{2}{3}}}, \\ r^2 \frac{\partial f}{\partial r} &= -3\pi N^{1/3} \tilde{R} \frac{\left(1 - \frac{f+\sin f}{\pi}\right)^{\frac{4}{3}}}{1+\cos f}, \\ \frac{\partial r^3}{\partial f} &= -\frac{N\tilde{R}^3}{\pi}(1+\cos f), \end{aligned} \tag{3.36}$$

and can write the leading-order correction to the energy divided by $2\pi\epsilon$ as

$$\begin{aligned} \frac{M_{\mathrm{LO}}^{(1,2)}(N)}{2\pi} = {} & 3\pi c_2 \tilde{R} N^{1/3} a_1 + \frac{c_2 \tilde{R}(1+N^2) N^{1/3}}{3\pi} a_2 + \frac{3\pi c_4 (1+N^2)}{\tilde{R} N^{1/3}} a_3 + \frac{c_4 N^{5/3}}{3\pi\tilde{R}} a_4 \\ & + \frac{m_\pi^2 N \tilde{R}^3}{3}, \end{aligned} \tag{3.37}$$

where we have defined the integrals

$$
\begin{aligned}
a_1 &\equiv \int_0^\pi \frac{\left(1-\frac{f+\sin f}{\pi}\right)^{\frac{4}{3}}}{1+\cos f}\,\mathrm{d}f \simeq 0.4699,\\
a_2 &\equiv \int_0^\pi \frac{\sin^2 f(1+\cos f)}{\left(1-\frac{f+\sin f}{\pi}\right)^{\frac{2}{3}}}\,\mathrm{d}f \simeq 4.824,\\
a_3 &\equiv \int_0^\pi \frac{\sin^2 f\left(1-\frac{f+\sin f}{\pi}\right)^{\frac{2}{3}}}{1+\cos f}\,\mathrm{d}f \simeq 0.5167,\\
a_4 &\equiv \int_0^\pi \frac{\sin^4 f(1+\cos f)}{\left(1-\frac{f+\sin f}{\pi}\right)^{\frac{4}{3}}}\,\mathrm{d}f \simeq 16.327,
\end{aligned}
\tag{3.38}
$$

and

$$
R = \sqrt[3]{N}\tilde{R}, \qquad \tilde{R} = \sqrt[3]{\frac{3\pi\sqrt{2c_6}}{\mu}}. \tag{3.39}
$$

Notice that the pion mass term is linearly proportional to N and does not affect $N_\star$. Setting $c_4 := 0$, we find the minimum of the leading-order correction per N as

$$
N_\star^{(1,2)} = \sqrt{\frac{1}{2}+\frac{9\pi^2 a_1}{2a_2}} \simeq 2.197. \tag{3.40}
$$

Explicit checks find that $M_{\rm LO}(2)/2 < M_{\rm LO}(3)/3 < M_{\rm LO}(4)/4 < M_{\rm LO}(1) < M_{\rm LO}(5)/5$. We also explicitly find that $M_{\rm LO}(3) < 2M_{\rm LO}(2) + M_{\rm LO}(1)$. Setting instead $c_2 := 0$, we find the minimum of the leading-order correction per N as

$$
N_\star^{(1,2)} = \sqrt{\frac{2}{1+\frac{a_4}{9\pi^2 a_3}}} \simeq 1.215. \tag{3.41}
$$

Explicit checks find that $M_{\rm LO}(1) < M_{\rm LO}(N)/N$, for any $N > 1$. In general, $N_\star^{(1,2)}$ is a function of the ratio $c_4/(c_2\tilde{R}^2)$ and the equation for $N_\star$ reads

$$
-\frac{3\pi a_1}{N^{4/3}} + \frac{a_2(2N^2-1)}{3\pi N^{4/3}} + 3\pi a_3 x\left(1-\frac{2}{N^2}\right) + \frac{x a_4}{3\pi} = 0, \qquad x := \frac{c_4}{c_2\tilde{R}^2}. \tag{3.42}
$$

The solution to the equation, namely $N_\star^{(1,2)}$, is shown in figure 1 as a function of x.

Finally, we will consider the case of the potential (2.18) with $(s,p) = (2,2)$, for which we have the Bogomol'nyi mass (2.45) and BPS solution (2.37), and we further have

$$
f_r^2 = 9\pi^2\frac{r^4}{R^6}, \qquad \sin^2 f = \sin^2\left(\frac{\pi r^3}{R^3}\right), \tag{3.43}
$$

so now the LO energy is convergent and we can write the LO energy divided by $2\pi\epsilon$ as

$$
\begin{aligned}
\frac{M_{\rm LO}^{(2,2)}}{2\pi} = {}& \frac{9\pi^2 c_2\tilde{R}N^{1/3}}{7} + c_2(1+N^2)\Upsilon_1\tilde{R}N^{1/3} + c_4(1+N^2)\frac{9\pi^2\Upsilon_2}{\tilde{R}N^{1/3}} + \frac{c_4 N^{5/3}\Upsilon_3}{\tilde{R}}\\
&+ \frac{2m_\pi^2 N\tilde{R}^3}{3},
\end{aligned}
\tag{3.44}
$$

JHEP11(2022)092

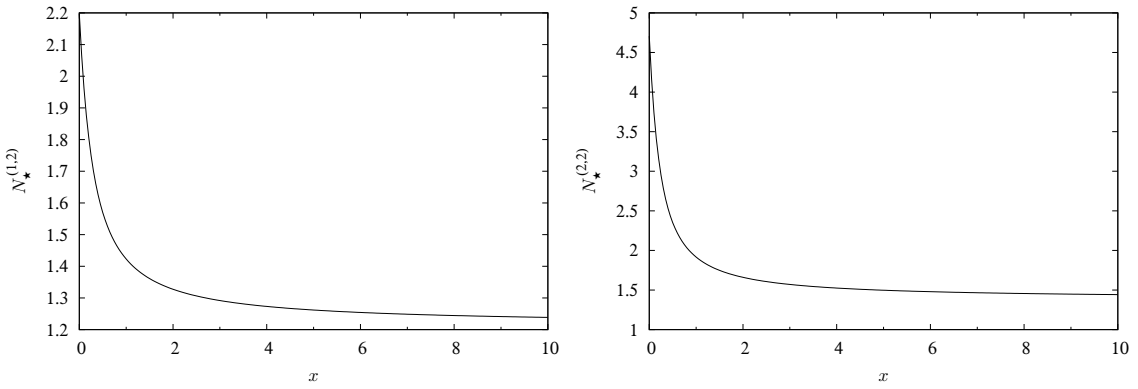

Figure 1. $N_\star^{(1,2)}$ and $N_\star^{(2,2)}$ as functions of $x = \frac{c_4}{c_2\tilde{R}^2}$.

where

$$R = \sqrt[3]{N}\tilde{R}, \qquad \tilde{R} = \sqrt[3]{\frac{6\pi\sqrt{c_6}}{\mu}}, \tag{3.45}$$

$$\Upsilon_1 = \int_0^1 \sin^2(\pi x^3)\, \mathrm{d}x \simeq 0.29303, \tag{3.46}$$

$$\Upsilon_2 = \int_0^1 \sin^2(\pi x^3) x^4\, \mathrm{d}x \simeq 0.103303, \tag{3.47}$$

$$\Upsilon_3 = \int_0^1 \frac{\sin^4(\pi x^3)}{x^2}\, \mathrm{d}x \simeq 0.370701. \tag{3.48}$$

Notice again that the contribution from the pion mass term is linear in N and hence will not affect $N_\star$. If we set $c_4 := 0$, the LO mass per N has a minimum at

$$N_\star^{(2,2)} = \sqrt{\frac{1}{2} + \frac{9\pi^2}{14\Upsilon_1}} \simeq 4.707. \tag{3.49}$$

Explicit checks find that $M_{\mathrm{LO}}(5)/5 < M_{\mathrm{LO}}(4)/4 < M_{\mathrm{LO}}(6)/6 < M_{\mathrm{LO}}(7)/7 < M_{\mathrm{LO}}(3)/3 < M_{\mathrm{LO}}(8)/8 < M_{\mathrm{LO}}(9)/9 < M_{\mathrm{LO}}(2)/2 < M_{\mathrm{LO}}(10)/10 < M_{\mathrm{LO}}(11)/11 < M_{\mathrm{LO}}(12)/12 < M_{\mathrm{LO}}(13)/13 < M_{\mathrm{LO}}(14)/14 < M_{\mathrm{LO}}(15)/15 < M_{\mathrm{LO}}(1) < M_{\mathrm{LO}}(16)/16$. This means that there are many generalized-restricted harmonic solutions that have less energy per baryon number than the spherically symmetric 1-Skyrmions. This is quite surprising.

On the other hand, if we set $c_2 := 0$, the LO mass per N has a minimum given by

$$N_\star^{(2,2)} = \sqrt{\frac{2}{1 + \frac{\Upsilon_3}{9\pi^2\Upsilon_2}}} \simeq 1.386, \tag{3.50}$$

and explicit checks verify that $\frac{M_{\mathrm{LO}}(N)}{N} < \frac{M_{\mathrm{LO}}(N+1)}{N+1}$ for all $N = 1, 2, \ldots$ In general, $N_\star^{(2,2)}$ is a function of the ratio $c_4/(c_2\tilde{R}^2)$ and the equation for $N_\star$ reads

$$-\frac{3\pi}{7} + \frac{\Upsilon_1(2N^2-1)}{3\pi} + \frac{3\pi x\Upsilon_2(N^2-2)}{N^{2/3}} + \frac{N^{4/3}x\Upsilon_3}{3\pi} = 0, \qquad x := \frac{c_4}{c_2\tilde{R}^2}. \tag{3.51}$$

The solution to this equation, i.e. $N_\star^{(2,2)}$, is shown in figure 1 as a function of x.

JHEP11(2022)092

To summarize, we have found that for the potentials (2.18) with $(s,p) = (2,1)$ and $(s,p) = (2,2)$, setting $c_4 := 0$, we have solutions with lower energy per N to leading order in ϵ for $N > 1$, which means that the spherically symmetric 1-Skyrmion is at best metastable in the near-BPS limit (for those potentials). On the other hand, for $c_2 := 0$ and $(s,p) = (2,1), (2,2), (1,1), (1,2)$, we have found that the 1-Skyrmion is the energetically preferred solution.

In the situation with both $c_2 > 0$ and $c_4 > 0$, for the cases $(s,p) = (1,2)$ and $(s,p) = (2,2)$, the value of $N_\star$ rapidly reaches ~ 1 for $c_4 \gg c_2 R^2$ (see figure 1). As a consequence, in the following of the paper, we impose the constraint $c_4 \gg c_2 R^2$ in order to build stable nuclei made of $B = 1+1+1+\cdots$ Skyrmions. Note that the addition of $m_\pi > 0$ does not change $N_\star$.

3.3 NLO and N^{2}LO corrections

We now consider the next-to-leading order (NLO) and next-to-next-to-leading order (N^{2}LO) corrections to the energy, meaning that we have to take into account the corrections of order $\mathcal{O}(\epsilon^2)$ and $\mathcal{O}(\epsilon^3)$. The reason for having to consider the perturbed Lagrangian up to $\mathcal{O}(\epsilon^3)$ has been discussed in ref. [23] for the 2-dimensional case and it is strictly related with the choice of the compacton-type solution as the background field. Indeed, since the compacton field is constant outside its finite domain, all the terms that contain derivatives of the background field vanish outside said region. As a result, the first order of the field expansion vanishes outside the compacton domain and then, iterating the perturbative scheme, all orders of the expansion vanish too. In other words, using the compacton solution as the zeroth order of the field expansion, the ordinary perturbation scheme fails. To avoid this problem, in ref. [23], both the quadratic order and the third order in ϵ have been considered together. In this way, at the price of harder analytical computations, the solution of the perturbed field exists even outside the compacton region and the perturbative method works. We adopt here the same strategy for the 3-dimensional case.

For the perturbative ϵ-expansion, we will again utilize the O(4) vector field $\Phi = (\Phi_0, \Phi_1, \Phi_2, \Phi_3)$ that is related to the SU(2) matrix, U as defined in eqs. (2.6) and (3.14). In this way, the computations are similar to the 2-dimensional case (in which the field is parameterized by an O(3) vector field). We will thus perform the perturbative expansion directly in the Φ field

$$\Phi = \Phi + \delta\Phi, \tag{3.52}$$

where Φ denotes here the BPS background solution and $\delta\Phi$ is a small perturbation. In this notation, the Lagrangian (2.1) with $\mathcal{L}_0$ given by eq. (2.18) now reads [40, 41]

$$\mathcal{L}_6 = \frac{1}{36}\eta_{\mu\mu'}\epsilon^{\mu\nu\rho\sigma}\epsilon^{abcd}\,\Phi^a\partial_\nu\Phi^b\partial_\rho\Phi^c\partial_\sigma\Phi^d\,\epsilon^{\mu'\nu'\rho'\sigma'}\epsilon_{efgh}\Phi^e\partial_{\nu'}\Phi^f\partial_{\rho'}\Phi^g\partial_{\sigma'}\Phi^h \tag{3.53}$$

$$= -\frac{1}{3}(\partial_\mu\Phi\cdot\partial^\nu\Phi)(\partial_\nu\Phi\cdot\partial^\rho\Phi)(\partial_\rho\Phi\cdot\partial^\mu\Phi) + \frac{1}{2}(\partial_\mu\Phi\cdot\partial^\nu\Phi)(\partial_\nu\Phi\cdot\partial^\mu\Phi)(\partial_\rho\Phi\cdot\partial^\rho\Phi) - \frac{1}{6}(\partial_\mu\Phi\cdot\partial^\mu\Phi)^3, \tag{3.54}$$

$$\mathcal{L}_0 = -V_{s,p} = -\frac{1}{sp}(1-(\Phi^a n^a)^s)^p, \tag{3.55}$$

JHEP11(2022)092

$$\mathcal{L}_2 = -\frac{1}{2}(\partial_\mu \Phi \cdot \partial^\mu \Phi) \tag{3.56}$$

$$\mathcal{L}_4 = \frac{1}{4}(\partial_\mu \Phi \cdot \partial^\nu \Phi)(\partial_\nu \Phi \cdot \partial^\mu \Phi) - \frac{1}{4}(\partial_\mu \Phi \cdot \partial^\mu \Phi)^2, \tag{3.57}$$

$$-V_{1,1} = -(1 - \Phi^a n^a), \tag{3.58}$$

$$\mathcal{L}_\lambda = \frac{\lambda}{2}(\Phi \cdot \Phi - 1), \tag{3.59}$$

where $n^a = \delta^{a0}$ is the vacuum of the theory and we use the convention $\epsilon^{0123} = 1$.

For the NLO and N^{2}LO corrections, we need to calculate the variation up to third order (in the fields) of the Lagrangian (2.1) (assuming that $\delta\Phi = \mathcal{O}(\epsilon)$)

$$\begin{aligned}
\mathcal{L}^{\text{perturb}}[\Phi, \delta\Phi] = & \frac{\partial \mathcal{L}}{\partial\lambda \partial \Phi^a}\bigg| \delta\lambda\, \delta\Phi^a + \frac{1}{2}\, \frac{\partial \mathcal{L}}{\partial\lambda \partial \Phi^a \partial \Phi^b}\bigg| \delta\lambda\, \delta\Phi^a\, \delta\Phi^b + \frac{\partial \mathcal{L}}{\partial \Phi^a}\bigg| \delta\Phi^a \\
& + \frac{1}{2}\frac{\partial^2 \mathcal{L}}{\partial \Phi^a \partial \Phi^b}\bigg| \delta\Phi^a \delta\Phi^b + \frac{1}{6}\frac{\partial^3 \mathcal{L}}{\partial \Phi^a \partial \Phi^b \partial \Phi^c}\bigg| \delta\Phi^a \delta\Phi^b \delta\Phi^c + \frac{\partial \mathcal{L}}{\partial \partial_\mu \Phi^a}\bigg| \partial_\mu \delta\Phi^a \\
& + \frac{1}{2}\frac{\partial^2 \mathcal{L}}{\partial \partial_\mu \Phi^a \partial \partial_\nu \Phi^b}\bigg| \partial_\mu \delta\Phi^a \partial_\nu \delta\Phi^b \\
& + \frac{1}{6}\frac{\partial^3 \mathcal{L}}{\partial \partial_\mu \Phi^a \partial \partial_\nu \Phi^b \partial \partial_\rho \Phi^c}\bigg| \partial_\mu \delta\Phi^a \partial_\nu \delta\Phi^b \partial_\rho \delta\Phi^c \\
= & \, \delta\lambda \left(\frac{1}{2}\delta\Phi \cdot \delta\Phi + \Phi \cdot \delta\Phi \right) + \mu^2 \Xi + \epsilon m_\pi^2 \delta\Phi^0 + \frac{\lambda_0}{2}\delta\Phi \cdot \delta\Phi - \epsilon J_a^\mu \partial_\mu \delta\Phi^a \\
& - \frac{1}{2} V_{ab}^{\mu\nu} \partial_\mu \delta\Phi^a \partial_\nu \delta\Phi^b - \frac{1}{6}\Gamma_{abc}^{\mu\nu\rho} \partial_\mu \delta\Phi^a \partial_\nu \delta\Phi^b \partial_\rho \delta\Phi^c,
\end{aligned} \tag{3.60}$$

where the symbol $|$ means that the expression to the left is evaluated on the background field Φ, and we have defined the symbols

$$\begin{aligned}
\Xi = & -\frac{s}{2}(p-1)(1-(\Phi^0)^s)^{p-2}(\Phi^0)^{2s-2}(\delta\Phi^0)^2 + \frac{1}{2}(s-1)(1-(\Phi^0)^s)^{p-1}(\Phi^0)^{s-2}(\delta\Phi^0)^2 \\
& + \frac{1}{6}s^2(p-1)(p-2)(1-(\Phi^0)^s)^{p-3}(\Phi^0)^{3s-3}(\delta\Phi^0)^3 \\
& - \frac{1}{2}s(s-1)(p-1)(1-(\Phi^0)^s)^{p-2}(\Phi^0)^{2s-3}(\delta\Phi^0)^3 \\
& \frac{1}{6}(s-1)(s-2)(1-(\Phi^0)^s)^{p-1}(\Phi^0)^{s-3}(\delta\Phi^0)^3,
\end{aligned} \tag{3.61}$$

$$J_a^\mu = c_2 \partial^\mu \Phi^a - c_4(\partial^\mu \Phi \cdot \partial^\nu \Phi)\partial_\nu \Phi^a + c_4(\partial_\nu \Phi \cdot \partial^\nu \Phi)\partial^\mu \Phi^a, \tag{3.62}$$

$$V_{ab}^{\mu\nu} = V_{0ab}^{\mu\nu} + \epsilon V_{1ab}^{\mu\nu}, \tag{3.63}$$

$$\begin{aligned}
V_{0ab}^{\mu\nu} = & \, 2c_6(\partial_\rho \Phi \cdot \partial_\sigma \Phi)\partial^\rho \Phi^a \partial^\sigma \Phi^b \eta^{\mu\nu} + 2c_6(\partial^\nu \Phi \cdot \partial_\rho \Phi)\partial^\rho \Phi^a \partial^\mu \Phi^b + 2c_6(\partial^\mu \Phi \cdot \partial^\nu \Phi)\partial_\rho \Phi^a \partial^\rho \Phi^b \\
& + 2c_6(\partial^\mu \Phi \cdot \partial_\rho \Phi)\partial^\nu \Phi^a \partial^\rho \Phi^b + 2c_6(\partial^\mu \Phi \cdot \partial_\rho \Phi)(\partial^\nu \Phi \cdot \partial^\rho \Phi)\delta^{ab} \\
& - 2c_6(\partial_\rho \Phi \cdot \partial^\rho \Phi)\partial_\sigma \Phi^a \partial^\sigma \Phi^b \eta^{\mu\nu} - 2c_6(\partial_\rho \Phi \cdot \partial^\rho \Phi)\partial^\nu \Phi^a \partial^\mu \Phi^b \\
& - 2c_6(\partial^\mu \Phi \cdot \partial^\nu \Phi)(\partial_\rho \Phi \cdot \partial^\rho \Phi)\delta^{ab} - 4c_6(\partial^\mu \Phi \cdot \partial_\rho \Phi)\partial^\rho \Phi^a \partial^\nu \Phi^b \\
& - 4c_6(\partial^\nu \Phi \cdot \partial_\rho \Phi)\partial^\mu \Phi^a \partial^\rho \Phi^b - c_6(\partial_\rho \Phi \cdot \partial_\sigma \Phi)(\partial^\rho \Phi \cdot \partial^\sigma \Phi)\eta^{\mu\nu}\delta^{ab} \\
& + 4c_6(\partial_\rho \Phi \cdot \partial^\rho \Phi)\partial^\mu \Phi^a \partial^\nu \Phi^b + c_6(\partial_\rho \Phi \cdot \partial^\rho \Phi)(\partial_\sigma \Phi \cdot \partial^\sigma \Phi)\eta^{\mu\nu}\delta^{ab},
\end{aligned} \tag{3.64}$$

JHEP11(2022)092

$$
\begin{aligned}
V^{\mu\nu}_{1ab} &= c_2\eta^{\mu\nu}\delta^{ab} + c_4(\partial_\rho\Phi\cdot\partial^\rho\Phi)\eta^{\mu\nu}\delta^{ab} + 2c_4\partial^\mu\Phi^a\partial^\nu\Phi^b - c_4(\partial^\mu\Phi\cdot\partial^\nu\Phi)\delta^{ab} - c_4\partial^\mu\Phi^b\partial^\nu\Phi^a \\
&\quad - c_4\partial_\rho\Phi^a\partial^\rho\Phi^b\eta^{\mu\nu}, \qquad (3.65)\\
\Gamma^{\mu\nu\rho}_{abc} &= 8c_6\partial^\mu\Phi^a\partial^\nu\Phi^b\partial^\rho\Phi^c + 2c_6\partial^\rho\Phi^a\partial^\mu\Phi^b\partial^\nu\Phi^c + 2c_6\partial^\nu\Phi^a\partial^\rho\Phi^b\partial^\mu\Phi^c - 4c_6\partial^\nu\Phi^a\partial^\mu\Phi^b\partial^\rho\Phi^c \\
&\quad - 4c_6\partial^\rho\Phi^a\partial^\nu\Phi^b\partial^\mu\Phi^c - 4c_6\partial^\mu\Phi^a\partial^\rho\Phi^b\partial^\nu\Phi^c \\
&\quad + c_6\eta^{\mu\nu}\big(2\partial^\rho\Phi^a\partial_\sigma\Phi^b\partial^\sigma\Phi^c + 2\partial_\sigma\Phi^a\partial^\rho\Phi^b\partial^\sigma\Phi^c - 4\partial_\sigma\Phi^a\partial^\sigma\Phi^b\partial^\rho\Phi^c\big) \\
&\quad + c_6\eta^{\mu\rho}\big(2\partial^\nu\Phi^a\partial_\sigma\Phi^b\partial^\sigma\Phi^c + 2\partial_\sigma\Phi^a\partial^\sigma\Phi^b\partial^\nu\Phi^c - 4\partial_\sigma\Phi^a\partial^\nu\Phi^b\partial^\sigma\Phi^c\big) \\
&\quad + c_6\eta^{\nu\rho}\big(2\partial_\sigma\Phi^a\partial^\mu\Phi^b\partial^\sigma\Phi^c + 2\partial_\sigma\Phi^a\partial^\sigma\Phi^b\partial^\mu\Phi^c - 4\partial^\mu\Phi^a\partial_\sigma\Phi^b\partial^\sigma\Phi^c\big) \\
&\quad + c_6\delta^{ab}\big(2(\partial^\nu\Phi\cdot\partial^\rho\Phi)\partial^\mu\Phi^c + 2(\partial^\mu\Phi\cdot\partial^\rho\Phi)\partial^\nu\Phi^c - 4(\partial^\mu\Phi\cdot\partial^\nu\Phi)\partial^\rho\Phi^c\big) \\
&\quad + c_6\delta^{ac}\big(2(\partial^\mu\Phi\cdot\partial^\nu\Phi)\partial^\rho\Phi^b + 2(\partial^\nu\Phi\cdot\partial^\rho\Phi)\partial^\mu\Phi^b - 4(\partial^\mu\Phi\cdot\partial^\rho\Phi)\partial^\nu\Phi^b\big) \\
&\quad + c_6\delta^{bc}\big(2(\partial^\mu\Phi\cdot\partial^\nu\Phi)\partial^\rho\Phi^a + 2(\partial^\mu\Phi\cdot\partial^\rho\Phi)\partial^\nu\Phi^a - 4(\partial^\nu\Phi\cdot\partial^\rho\Phi)\partial^\mu\Phi^a\big) \\
&\quad + 4c_6\delta^{ab}\eta^{\mu\nu}\big((\partial_\sigma\Phi\cdot\partial^\sigma\Phi)\partial^\rho\Phi^c - (\partial^\rho\Phi\cdot\partial_\sigma\Phi)\partial^\sigma\Phi^c\big) \\
&\quad + 2c_6\delta^{ab}\eta^{\mu\rho}\big((\partial^\nu\Phi\cdot\partial_\sigma\Phi)\partial^\sigma\Phi^c - (\partial_\sigma\Phi\cdot\partial^\sigma\Phi)\partial^\nu\Phi^c\big) \\
&\quad + 2c_6\delta^{ab}\eta^{\nu\rho}\big((\partial^\mu\Phi\cdot\partial_\sigma\Phi)\partial^\sigma\Phi^c - (\partial_\sigma\Phi\cdot\partial^\sigma\Phi)\partial^\mu\Phi^c\big) \\
&\quad + 2c_6\delta^{ac}\eta^{\mu\nu}\big((\partial^\rho\Phi\cdot\partial_\sigma\Phi)\partial^\sigma\Phi^b - (\partial_\sigma\Phi\cdot\partial^\sigma\Phi)\partial^\rho\Phi^b\big) \\
&\quad + 4c_6\delta^{ac}\eta^{\mu\rho}\big((\partial_\sigma\Phi\cdot\partial^\sigma\Phi)\partial^\nu\Phi^b - (\partial^\nu\Phi\cdot\partial_\sigma\Phi)\partial^\sigma\Phi^b\big) \\
&\quad + 2c_6\delta^{ac}\eta^{\nu\rho}\big((\partial^\mu\Phi\cdot\partial_\sigma\Phi)\partial^\sigma\Phi^b - (\partial_\sigma\Phi\cdot\partial^\sigma\Phi)\partial^\mu\Phi^b\big) \\
&\quad + 2c_6\delta^{bc}\eta^{\mu\nu}\big((\partial^\rho\Phi\cdot\partial_\sigma\Phi)\partial^\sigma\Phi^a - (\partial_\sigma\Phi\cdot\partial^\sigma\Phi)\partial^\rho\Phi^a\big) \\
&\quad + 2c_6\delta^{bc}\eta^{\mu\rho}\big((\partial^\nu\Phi\cdot\partial_\sigma\Phi)\partial^\sigma\Phi^a - (\partial_\sigma\Phi\cdot\partial^\sigma\Phi)\partial^\nu\Phi^a\big) \\
&\quad + 4c_6\delta^{bc}\eta^{\nu\rho}\big((\partial_\sigma\Phi\cdot\partial^\sigma\Phi)\partial^\mu\Phi^a - (\partial^\mu\Phi\cdot\partial_\sigma\Phi)\partial^\sigma\Phi^a\big). \qquad (3.66)
\end{aligned}
$$

In the perturbed Lagrangian we have consistently expanded the Lagrange multiplier λ as $\lambda \to \lambda_0 + \delta\lambda$, where λ_0 is the Lagrange multiplier solution of the background BPS model

$$
\begin{aligned}
\lambda_0 = &-2c_6(\partial^\nu\Phi\cdot\partial^\rho\Phi)(\partial_\rho\Phi\cdot\partial^\mu\Phi)(\partial_\mu\partial_\nu\Phi\cdot\Phi) + c_6(\partial_\nu\Phi\cdot\partial^\rho\Phi)(\partial_\rho\Phi\cdot\partial^\nu\Phi)(\partial^2\Phi\cdot\Phi) \\
&+ 2c_6(\partial_\rho\Phi\cdot\partial^\rho\Phi)(\partial^\mu\Phi\cdot\partial^\nu\Phi)(\partial_\mu\partial_\nu\Phi\cdot\Phi) - c_6(\partial_\mu\Phi\cdot\partial^\mu\Phi)^2(\partial^2\Phi\cdot\Phi) \\
&- \mu^2\big(1-(\Phi^0)^s\big)^{p-1}(\Phi^0)^s. \qquad (3.67)
\end{aligned}
$$

The role of $\delta\lambda$ is to ensure that the norm of the unit four-vector Φ does not change up to the accuracy of the perturbation order. Indeed, the equation of motion for the perturbed Lagrangian with respect to $\delta\lambda$ gives

$$
\left(\frac{1}{2}\delta\Phi^2 + \Phi\cdot\delta\Phi\right) = 0. \qquad (3.68)
$$

In order to solve the above constraint equation, it will prove convenient to use differential forms with $\delta\Phi = \delta\Phi^a \mathrm{d}y^a$ a 1-form on a 4-dimensional space in which the target space is embedded, and a natural Ansatz is to take $\delta\Phi = *(\Delta\wedge\Phi) + \omega$ with ω a 1-form (to be determined), since the first term is transverse to Φ by construction. Δ is a 2-form, which will parametrize the tangent directions to the target space, as we will see later. Computing

JHEP11(2022)092

the terms in eq. (3.68), we have

$$\frac{1}{2}(\delta\Phi,\delta\Phi)=\frac{1}{2}|\Delta\wedge\Phi|^2+\frac{1}{2}|\omega|^2, \tag{3.69}$$

$$(\Phi,\delta\Phi)=(\Phi,\omega), \tag{3.70}$$

with $(\ ,\ )$ the inner product. The cross terms in eq. (3.69) vanish due to antisymmetry:

$$\frac{1}{2}\int *(\Delta\wedge\Phi)\wedge *\omega+\frac{1}{2}\int\omega\wedge\Delta\wedge\Phi=-\frac{1}{2}\int\omega\wedge\Delta\wedge\Phi+\frac{1}{2}\int\omega\wedge\Delta\wedge\Phi=0, \tag{3.71}$$

since $*^2=-1$ for a 1-form in 4 dimensions. Writing out eq. (3.68), we have

$$\begin{aligned}&\frac{1}{2}\int\Delta\wedge\Phi\wedge *(\Delta\wedge\Phi)+\int\Phi\wedge *\omega+\frac{1}{2}\int\omega\wedge *\omega\\&=\int\Phi\wedge\left(\frac{1}{2}\Delta\wedge *(\Delta\wedge\Phi)+*\omega\right)+\frac{1}{2}\int\omega\wedge *\omega=0.\end{aligned} \tag{3.72}$$

Setting the parenthesis to zero yields the 1-form solution

$$\delta\Phi=*(\Delta\wedge\Phi)+\frac{1}{2}*\Delta\wedge *(\Delta\wedge\Phi). \tag{3.73}$$

which is consistent, because $|\omega|^2$ is of order Δ^4 and hence ϵ^4. Writing out the components of $\delta\Phi$, we get

$$\delta\Phi^a=\epsilon^{abcd}\Delta_{bc}\Phi^d+\frac{1}{2}\epsilon^{abcd}\Delta_{bc}\epsilon^{defg}\Delta_{ef}\Phi^g. \tag{3.74}$$

The solution can also be viewed as due to the standard Gram-Schmidt orthonormalization algorithm to second order. The norm of the vector field Φ is therefore

$$\Phi^a\Phi^a=1+\mathcal{O}(\epsilon^4), \tag{3.75}$$

as we request. Moreover, by using the Ansatz (3.74), it is clear that the contribution to the energy of the terms multiplied by $\delta\lambda$ will be of order $\mathcal{O}(\epsilon^5)$ and then we can neglect them in the final calculation of the total energy. The job of $\delta\lambda$ was indeed just to cast the form of the perturbation as found in eq. (3.74).

3.4 Axially symmetric perturbations

It will prove convenient to define the following basis vectors

$$\Phi_r=\begin{pmatrix}-\sin f(r)\\ \cos f(r)\sin(\theta)\cos(N\varphi)\\ \cos f(r)\sin(\theta)\sin(N\varphi)\\ \cos f(r)\cos(\theta)\end{pmatrix},\quad \Phi_\theta=\begin{pmatrix}0\\ \cos(\theta)\cos(N\varphi)\\ \cos(\theta)\sin(N\varphi)\\ -\sin(\theta)\end{pmatrix},\quad \Phi_\varphi=\begin{pmatrix}0\\ -\sin(N\varphi)\\ \cos(N\varphi)\\ 0\end{pmatrix}, \tag{3.76}$$

in terms of the background field solution with axial symmetry

$$\Phi=\begin{pmatrix}\cos f(r)\\ \sin f(r)\sin(\theta)\cos(N\varphi)\\ \sin f(r)\sin(\theta)\sin(N\varphi)\\ \sin f(r)\cos(\theta)\end{pmatrix}, \tag{3.77}$$

JHEP11(2022)092

for which the perturbation tensor for axially symmetric perturbations are pointed in the direction of the tensor product of the θ and φ directions, hence we have

$$\Delta^r_{ab} = -\Phi^\theta_a \Phi^\varphi_b \, \delta f(r), \tag{3.78}$$

and therefore the perturbation field for axially symmetric perturbations reads

$$\delta\Phi = \begin{pmatrix} -\sin f - \frac{1}{2}\cos f \delta f \\ \sin\theta\cos(N\varphi)\left(\cos f - \frac{1}{2}\sin f\delta f\right) \\ \sin\theta\sin(N\varphi)\left(\cos f - \frac{1}{2}\sin f\delta f\right) \\ \cos\theta\left(\cos f - \frac{1}{2}\sin f\delta f\right) \end{pmatrix} \delta f. \tag{3.79}$$

Writing out the total field, we have

$$\begin{aligned} \Phi &= \Phi + \delta\Phi \\ &= \begin{pmatrix} \cos f \\ \sin f\sin(\theta)\cos(N\varphi) \\ \sin f\sin(\theta)\sin(N\varphi) \\ \sin f\cos(\theta) \end{pmatrix} + \begin{pmatrix} -\sin f \\ \cos f\sin\theta\cos(N\varphi) \\ \cos f\sin\theta\sin(N\varphi) \\ \cos f\cos\theta \end{pmatrix}\delta f - \begin{pmatrix} \cos f \\ \sin f\sin\theta\cos(N\varphi) \\ \sin f\sin\theta\sin(N\varphi) \\ \sin f\cos\theta \end{pmatrix}\frac{\delta f^2}{2} \\ &\simeq \begin{pmatrix} \cos(f+\delta f) \\ \sin(f+\delta f)\sin(\theta)\cos(N\varphi) \\ \sin(f+\delta f)\sin(\theta)\sin(N\varphi) \\ \sin(f+\delta f)\cos(\theta) \end{pmatrix} + \mathcal{O}(\delta f^3). \end{aligned} \tag{3.80}$$

It is hence clear that the perturbation preserves the length of the field Φ, as any change in the function f does not change the length of the vector field Φ.

Restricting to a radial perturbation in the profile function, $\delta f = \delta f(r)$, we can write the perturbation energy as

$$\mathcal{E}^{\text{perturb}}(f,\delta f) = \mathcal{E}^{\text{perturb}}_2(f,\delta f) + \mathcal{E}^{\text{perturb}}_{3,\text{quad}}(f,\delta f) + \mathcal{E}^{\text{perturb}}_{3,\text{cubic}}(f,\delta f), \tag{3.81}$$

with

$$\begin{aligned} \mathcal{E}^{\text{perturb}}_2(f,\delta f) = {} & \frac{\mu^2}{2}\cos^{s-2} f\left(1-\cos^s f\right)^{p-2}(1-s+(sp-1)\cos^s f)\sin^2(f)\delta f^2 \\ & + \frac{\mu^2}{2}\cos^s f\left(1-\cos^s f\right)^{p-1}\delta f^2 - \frac{2c_6N^2}{r^4}\sin^2 f(4\sin^2 f-3)f_r^2\delta f^2 \\ & + \epsilon m_\pi^2\sin(f)\delta f + \epsilon c_2 f_r\delta f_r + \frac{\epsilon c_2(1+N^2)}{2r^2}\sin(2f)\delta f \\ & + \frac{\epsilon c_4(1+N^2)}{2r^2}\sin(2f)f_r^2\delta f + \frac{\epsilon c_4N^2}{r^4}\sin^2 f\sin(2f)\delta f \\ & + \frac{\epsilon c_4(1+N^2)}{r^2}\sin^2(f)f_r\delta f_r + \frac{c_6N^2}{r^4}\sin^4(f)\delta f_r^2 \\ & + \frac{4c_6N^2}{r^4}\sin^2 f\sin(2f)f_r\delta f\delta f_r, \end{aligned} \tag{3.82}$$

JHEP11(2022)092

for the NLO terms,

$$\begin{aligned}\mathcal{E}^{\text{perturb}}_{3,\text{quad}}(f,\delta f) = {}& \frac{\epsilon m_\pi^2}{2}\cos(f)\delta f^2 + \frac{\epsilon c_2}{2}\delta f_r^2 + \frac{\epsilon c_2(1+N^2)}{2r^2}\cos(2f)\delta f^2 \\ & - \frac{\epsilon c_4 N^2}{r^4}\sin^2 f(4\sin^2 f - 3)\delta f^2 + \frac{\epsilon c_4(1+N^2)}{2r^2}\cos(2f) f_r^2 \delta f^2 \\ & + \frac{\epsilon c_4(1+N^2)}{2r^2}\sin^2(f)\delta f_r^2 + \frac{\epsilon c_4(1+N^2)}{r^2}\sin(2f) f_r \delta f \delta f_r, \end{aligned} \tag{3.83}$$

for the NNLO terms quadratic in δf and

$$\begin{aligned}\mathcal{E}^{\text{perturb}}_{3,\text{cubic}}(f,\delta f) = {}& \frac{\mu^2}{2}\cos^{s-1} f(1-\cos^s f)^{p-2}(1 - s + (sp-1)\cos^s f)\sin(f)\delta f^3 \\ & + \frac{\mu^2}{6}\cos^{s-3} f(1-\cos^s f)^{p-3}\Big(2 - 3s + s^2 + (s-1)(4 + (1-3p)s)\cos^s f \\ & \qquad + (sp-2)(sp-1)\cos^{2s} f\Big)\sin^3(f)\delta f^3 \\ & - \frac{c_6 N^2}{r^4}(5\sin^2 f - 2)\sin(2f) f_r^2 \delta f^3 - \frac{3c_6 N^2}{r^4}\sin^2(f)(5\sin^2 f - 4) f_r \delta f^2 \delta f_r \\ & + \frac{2c_6 N^2}{r^4}\sin^2 f \sin(2f)\delta f \delta f_r^2, \end{aligned} \tag{3.84}$$

for the NNLO terms cubic in δf.

Outside the support of the compacton, $f = f_r = 0$ and hence the perturbation energy reduces to

$$\mathcal{E}^{\text{perturb, outside}}(f,\delta f) = \epsilon c_2\left(\frac{1}{2}\delta f_r^2 + \frac{1+N^2}{2}\frac{\delta f^2}{r^2} + \frac{m_\pi^2}{2c_2}\delta f^2\right). \tag{3.85}$$

The problem simplifies for spherical symmetry for which $N = 1$, since the boundary of the compacton becomes a sphere of radius R, hence simplifying drastically the boundary conditions for the outside perturbations. The corresponding equation of motion is the modified spherical Bessel equation

$$r^2\delta f_{rr} + 2r\delta f_r - 2\delta f - \frac{m_\pi^2 r^2}{c_2}\delta f = 0, \tag{3.86}$$

which in turn has the analytic solution being the first modified spherical Bessel function of the second kind

$$\delta f = \alpha k_1\left(\frac{m_\pi r}{\sqrt{c_2}}\right) = \alpha e^{-\frac{m_\pi r}{\sqrt{c_2}}}\left(\frac{\sqrt{c_2}}{m_\pi r} + \frac{c_2}{m_\pi^2 r^2}\right), \qquad \alpha > 0. \tag{3.87}$$

The perturbation outside of the compacton is thus a free massive boson with the mass of the pion, as is expected on physical grounds.

In order to perform numerical calculations with the axially symmetric Ansatz and $\delta f = \delta f(r)$, we actually need to pick a BPS background for which the leading order energy correction is minimized for $N = 1$, and it is furthermore needed that the derivative of the BPS solution is finite at the compacton radius; these constraints leave us only with the two

JHEP11(2022)092

cases $(s,p)=(1,2)$ and $(s,p)=(2,2)$, both with $c_4 \gg c_2 R^2$ (since we need $N_\star \approx 1$ for the spherically symmetric solution to be a minimizer of the energy functional, see figure 1). On the other hand, it is necessary that $c_2 \neq 0$, in order for the tail of the perturbation to exist outside of the compacton. The reason that it is necessary to have a finite derivative of the BPS profile function at the compacton radius ($f_r(R)$) is that we will have to impose a cusp condition on the perturbative computation, which becomes nontrivial if the condition has to cancel an infinite negative derivative. In this paper, we will consider only the case of the BPS potential $(s,p)=(1,2)$, whereas we leave the case $(s,p)=(2,2)$ for a future work.

3.4.1 $(s,p)=(1,2)$

Considering the potential (2.18) with $(s,p)=(1,2)$, which has Bogomol'nyi mass (2.43) and BPS solution (2.31), we can analytically determine the derivative of the BPS solution at the compacton radius R:

$$f_r(R) = -\frac{3\pi}{2R}, \tag{3.88}$$

and hence we need to impose the following condition on the perturbation field

$$\delta f_r(R^-) - \delta f_r(R^+) = \frac{3\pi}{2R}, \tag{3.89}$$

with R given in eq. (2.32). Using the analytic solution (3.87), we have

$$\begin{aligned}\delta f_r(R^-) &= \frac{3\pi}{2R} - \frac{\alpha e^{-\frac{m_\pi R}{\sqrt{c_2}}}}{R}\left(1+\frac{2\sqrt{c_2}}{m_\pi R}+\frac{2c_2}{m_\pi^2 R^2}\right) \\ &= \frac{3\pi}{2R} - \frac{\delta f(R^-)}{R}\left(1+\frac{m_\pi R}{\sqrt{c_2}}+\frac{1}{1+\frac{m_\pi R}{\sqrt{c_2}}}\right),\end{aligned} \tag{3.90}$$

which is a Robin-type of boundary condition.

In figure 2 is shown the profile function $f(r)$ for the $N=1$ spherically symmetric Skyrmion with $\epsilon = 0.01$ for various values of $m_\pi/\sqrt{c_2}$. The perturbative scheme (orange curves) is compared to the exact numerical results (black curves). The cusp in the perturbative solution is imposed by using the condition (3.90). For $c_4 = 0$ the perturbative scheme captures well the true solution for $m_\pi/\sqrt{c_2} = 2$, but not quite yet for large $c_4 = 8$, whereas it works well for large $c_4 = 8$ with $m_\pi/\sqrt{c_2} = 3$ being slightly large. We found in the previous section that $c_4 \gg c_2 R^2$ is necessary for the spherically symmetric Skyrmion to be the true minimizer of the energy functional, which is the reason for choosing $c_4 = 8 \gg (3\pi)^{2/3}$ for $c_6 = 1/2$ and $\mu = 1$.

From figure 2, we recognize that the perturbative method seems to better approximate the exact near-BPS solution when increasing the pion mass m_π. A possible explanation for that behavior is the following. The perturbative expansion of the Skyrme field (3.1) obviously works in the hypothesis of $\delta U \ll 1$, so that the truncation of the series is justified by neglecting the smaller and smaller higher orders. Therefore, the smaller the difference between the BPS background and the exact solution is, the smaller δU is required to be. In this work, the BPS background is a compacton so a suppressed near-BPS tail (obtained

JHEP11(2022)092

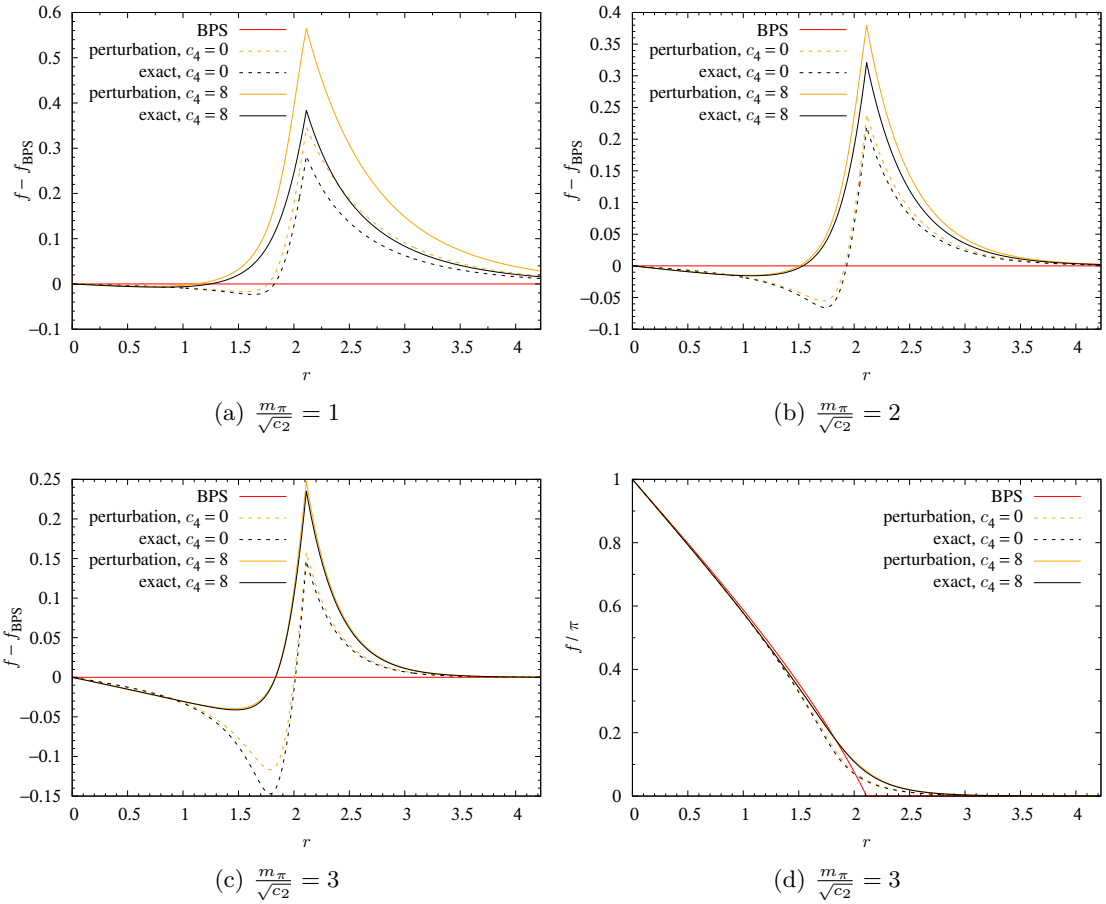

(a) $\frac{m_\pi}{\sqrt{c_2}} = 1$ (b) $\frac{m_\pi}{\sqrt{c_2}} = 2$

(c) $\frac{m_\pi}{\sqrt{c_2}} = 3$ (d) $\frac{m_\pi}{\sqrt{c_2}} = 3$

Figure 2. The profile function $f = f_{\rm BPS} + \delta f$ at N^{2}LO using linearized equation of motion in the BPS-Skyrme model with $(s, p) = (1, 2)$, for $c_4 = 0, 8$ and $m_\pi = 1, 2, 3$. The other parameters of the model has been set as: $c_2 = 1$, $c_6 = \frac{1}{2}$, $\mu = 1$ and hence the compacton radius $R = (3\pi)^{\frac{1}{3}} \simeq 2.112$.

with large m_π) should increase the accuracy of the perturbative method. Moreover, the linearization of the equation of motion operated at the NLO+N^{2}LO is better justified for δU very small, i.e. when the tail is well suppressed by a large m_π.

We are now ready to compare the energies of the exact numerical calculations with those of the perturbative scheme. The result is shown in figure 3. The NLO correction to the energy is calculated using eq. (3.82) which contributes with ϵ^2 to the energy and the N^{2}LO correction is calculated using the sum of eqs. (3.83) and (3.84) contributing of order ϵ^3.

Fitting the NLO and N^{2}LO corrections to the energy, we can write an approximate formula for the energy in the perturbative scheme (for $N = 1$, $c_2 = 1$, $m_\pi = 3$, $c_6 = \frac{1}{2}$ and $\mu = 1$):

$$\begin{aligned} E(\epsilon) &= M_{\rm BPS}^{(1,2)} + \epsilon M_{\rm LO}^{(1,2)} + \epsilon^2 M_{\rm NLO}^{(1,2)} + \epsilon^3 M_{\rm N^2LO}^{(1,2)} \\ &= 2\pi^2 + \epsilon\,(39.79 + 5.43 c_4) + \epsilon^2\,(-331.39 + 24.91 c_4) + \epsilon^3\,(229.87 - 20.36 c_4)\,. \end{aligned} \tag{3.91}$$

JHEP11(2022)092

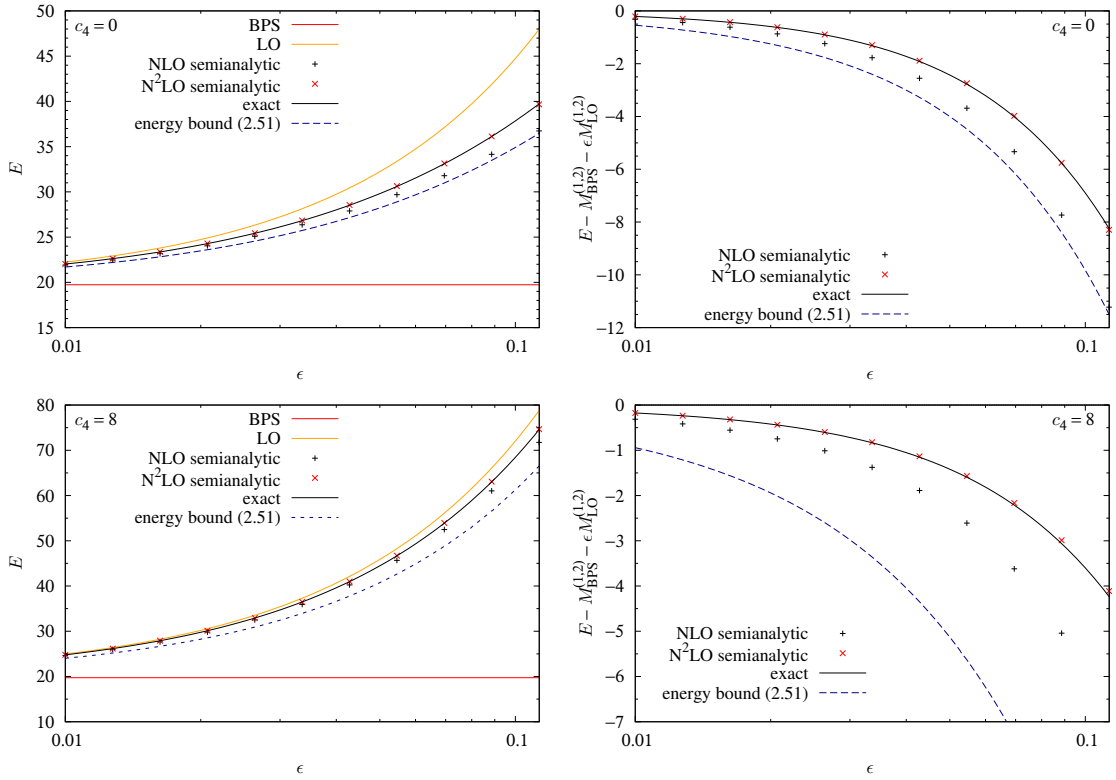

Figure 3. The mass of the Skyrmion in the perturbative ϵ-expansion as a function of ϵ on a logarithmic scale. The red solid line represents the BPS bound, the orange solid line is the LO correction to the energy, the black pluses are NLO corrections and finally the red crosses are N^{2}LO corrections. For comparison, the solid black line shows the exact ODE calculation. We also show the energy bound (A.8) with a blue-dashed line. The top row shows the case of $c_4 = 0$ and the bottom row shows $c_4 = 8$. In this figure $c_2 = 1$, $c_6 = \frac{1}{2}$, $\mu = 1$, $m_\pi = 3$, and $(s, p) = (1, 2)$.

The energy for different values of c_6 and μ (with modified values of m_π and c_2) can be recovered by a scaling argument of length and energy scales.

4 Binding energies

In order to calculate the binding energy between two $B = 1$ Skyrmions, we need to write down the energy with generic fluctuations turned on

$$\begin{aligned}\Delta_{ab} &= \Delta^r_{ab} + \Delta^\theta_{ab} + \Delta^\varphi_{ab} \\ &= -\Phi^\theta_a \Phi^\varphi_b \delta f(\mathbf{x}) - \Phi^\varphi_a \Phi^r_b \delta\theta(\mathbf{x}) - \Phi^r_a \Phi^\theta_b \delta\varphi(\mathbf{x}),\end{aligned} \tag{4.1}$$

and with δf not being restricted to being dependent only on the radial coordinate.

Geometrically, there is the direction Φ and only three tangent directions (Φ^r, Φ^θ and Φ^φ), since the target space is a 3-sphere. The tensor fluctuation (4.1) is the most general nonvanishing tensor that can be constructed out of tensor products of these vector directions (i.e. Φ, Φ^r, Φ^θ and Φ^φ); that is, any inclusion of Φ gives no contribution to $\delta\Phi$ of eq. (3.74).

JHEP11(2022)092

4.1 General fluctuation energy

The NLO + N^{2}LO energy density is given by

$$\mathcal{E}^{\text{perturb}}(f,\delta f,\delta\theta,\delta\varphi)=\mathcal{E}_2^{\text{perturb}}(f,\delta f,\delta\theta,\delta\varphi)+\mathcal{E}_{3,\text{quad}}^{\text{perturb}}(f,\delta f,\delta\theta,\delta\varphi)+\mathcal{E}_{3,\text{cubic}}^{\text{perturb}}(f,\delta f,\delta\theta,\delta\varphi), \tag{4.2}$$

with

$$\mathcal{E}_2^{\text{perturb}}=\epsilon X_{0\epsilon}^a\Omega^a+\sum_a\epsilon X_{1\epsilon}^a\hat{\mathbf{x}}_a^i\partial_i\Omega^a+\Omega^aY_0^{ab}\Omega^b+\Omega^aY_1^{abi}\partial_i\Omega^b+\partial_i\Omega^aY_2^{abij}\partial_j\Omega^b, \tag{4.3}$$

$$\mathcal{E}_{3,\text{quad}}^{\text{perturb}}=\epsilon\Omega^aY_{0\epsilon}^{ab}\Omega^b+\epsilon\Omega^aY_{1\epsilon}^{abi}\partial_i\Omega^b+\epsilon\partial_i\Omega^aY_{2\epsilon}^{abij}\partial_j\Omega^b, \tag{4.4}$$

$$\begin{aligned}\mathcal{E}_{3,\text{cubic}}^{\text{perturb}}&=Z_0^{abc}\Omega^a\Omega^b\Omega^c+\partial_i\Omega^aZ_1^{abci}\Omega^b\Omega^c+\partial_i\Omega^a\partial_j\Omega^bZ_2^{abcij}\Omega^c\\&\quad+\partial_i\Omega^a\partial_j\Omega^bZ_3^{abcijk}\partial_k\Omega^c,\end{aligned} \tag{4.5}$$

$i,j,k=1,2,3$ the spatial indices, $a,b,c=1,2,3$ the 3-vector indices, the definitions

$$\Omega^a=\begin{pmatrix}\delta f\\ \delta\theta\\ \delta\varphi\end{pmatrix},\quad \hat{\mathbf{x}}_1^i=\begin{pmatrix}\sin\theta\cos\varphi\\ \sin\theta\sin\varphi\\ \cos\theta\end{pmatrix},\quad \hat{\mathbf{x}}_2^i=\begin{pmatrix}\cos\theta\cos\varphi\\ \cos\theta\sin\varphi\\ -\sin\theta\end{pmatrix},\quad \hat{\mathbf{x}}_3^i=\begin{pmatrix}-\sin\varphi\\ \cos\varphi\\ 0\end{pmatrix}, \tag{4.6}$$

and the tensors

$$X_{0\epsilon}^a=\begin{pmatrix}\frac{c_2}{r^2}\sin(2f)+\frac{c_4}{r^2}\sin(2f)f_r^2+\frac{c_4}{r^4}\sin(2f)\sin^2f+m_\pi^2\sin f\\ \cot\theta\sin f\left(\frac{c_2}{r^2}+\frac{c_4}{r^4}\sin^2f+\frac{c_4}{r^2}f_r^2\right)\\ 0\end{pmatrix}, \tag{4.7}$$

$$X_{1\epsilon}^a=\begin{pmatrix}\left(c_2+\frac{2c_4}{r^2}\sin^2f\right)f_r\\ \frac{1}{r}\left(c_2+c_4f_r^2+\frac{c_4}{r^2}\sin^2f\right)\sin f\\ \frac{1}{r}\left(c_2+c_4f_r^2+\frac{c_4}{r^2}\sin^2f\right)\sin f\end{pmatrix}, \tag{4.8}$$

for the linear terms

$$Y_0^{ab}=\begin{pmatrix}Y_0^{11}&\frac{3c_6}{2r^4}\cot\theta\sin f\sin(2f)f_r^2&0\\ \frac{3c_6}{2r^4}\cot\theta\sin f\sin(2f)f_r^2&Y_0^{22}&0\\ 0&0&Y_0^{33}\end{pmatrix}, \tag{4.9}$$

$$\begin{aligned}Y_0^{11}&=-\frac{\mu^2}{4}\cos^{s-2}f(1-\cos^sf)^{p-2}\left(-2+2s\sin^2f+\cos^sf(2-2sp\sin^2f)\right)\\&\quad+\frac{2c_6}{r^4}(3-4\sin^2f)\sin^2(f)f_r^2,\end{aligned} \tag{4.10}$$

$$Y_0^{22}=\frac{\mu^2}{2}\cos^sf(1-\cos^sf)^{p-1}+\frac{c_6}{r^4}(\cot^2\theta-2\sin^2f)\sin^2(f)f_r^2, \tag{4.11}$$

$$Y_0^{33}=\frac{\mu^2}{2}\cos^sf(1-\cos^sf)^{p-1}-\frac{2c_6}{r^4}\sin^4(f)f_r^2, \tag{4.12}$$

$$Y_1^{abi}=\frac{c_6}{r^3}s_f^2f_r\begin{pmatrix}\frac{4}{r}s_{2f}\hat{\mathbf{x}}_1^i&6c_ff_r\hat{\mathbf{x}}_2^i&6c_ff_r\hat{\mathbf{x}}_3^i\\ \frac{4}{r}s_f(\hat{\mathbf{x}}_2^i+s_\theta^{-1}\delta^{i3})&(\frac{s_{2f}}{r}+\frac{4f_r}{t_\theta^2})\hat{\mathbf{x}}_1^i-\frac{4f_r}{s_\theta t_\theta}\delta^{i3}&\frac{2f_r}{t_\theta}\hat{\mathbf{x}}_3^i\\ 0&0&(\frac{s_{2f}}{r}+\frac{2f_r}{t_\theta^2})\hat{\mathbf{x}}_1^i-\frac{2f_r}{s_\theta t_\theta}\delta^{i3}\end{pmatrix}, \tag{4.13}$$

JHEP11(2022)092

$$Y_2^{abij} = \frac{c_6}{r^2} s_f^2 \begin{pmatrix} \frac{s_f^2}{r^2}\hat{\mathbf{x}}_1^i\hat{\mathbf{x}}_1^j & \frac{s_f f_r}{r}(\hat{\mathbf{x}}_1^i\hat{\mathbf{x}}_2^j + \epsilon^{ijk}\hat{\mathbf{x}}_3^k) & \frac{s_f f_r}{r}(\hat{\mathbf{x}}_1^i\hat{\mathbf{x}}_3^j - \epsilon^{ijk}\hat{\mathbf{x}}_2^k) \\ \frac{s_f f_r}{r}(\hat{\mathbf{x}}_2^i\hat{\mathbf{x}}_1^j - \epsilon^{ijk}\hat{\mathbf{x}}_3^k) & f_r^2\hat{\mathbf{x}}_2^i\hat{\mathbf{x}}_2^j & f_r^2(\hat{\mathbf{x}}_2^i\hat{\mathbf{x}}_3^j + \epsilon^{ijk}\hat{\mathbf{x}}_1^k) \\ \frac{s_f f_r}{r}(\hat{\mathbf{x}}_3^i\hat{\mathbf{x}}_1^j + \epsilon^{ijk}\hat{\mathbf{x}}_2^k) & f_r^2(\hat{\mathbf{x}}_3^i\hat{\mathbf{x}}_2^j - \epsilon^{ijk}\hat{\mathbf{x}}_1^k) & f_r^2\hat{\mathbf{x}}_3^i\hat{\mathbf{x}}_3^j \end{pmatrix}, \tag{4.14}$$

for the quadratic NLO terms

$$Y_{0\epsilon}^{11} = \frac{c_2}{r^2}\cos(2f) + \frac{c_4}{r^2}\cos(2f)f_r^2 + \frac{c_4}{r^4}\sin^2 f(3 - 4\sin^2 f) + \frac{m_\pi^2}{2}\cos f, \tag{4.15}$$

$$Y_{0\epsilon}^{22} = \frac{c_2}{2r^2}(\cos 2f + \cot^2\theta) - \frac{c_2}{2}f_r^2 + \frac{c_4}{2r^4}\sin^2 f(\cos(2f) + \cot^2\theta) - \frac{c_4}{2r^2}(3\sin^2 f - \cot^2\theta)f_r^2 + \frac{m_\pi^2}{2}\cos f, \tag{4.16}$$

$$Y_{0\epsilon}^{33} = \frac{c_2}{2r^2}(\cos 2f + \cot^2\theta) - \frac{c_2}{2}f_r^2 + \frac{c_4}{2r^4}\sin^2 f\cos 2f - \frac{c_4}{2r^2}(3\sin^2 f - \cot^2\theta)f_r^2 + \frac{m_\pi^2}{2}\cos f \tag{4.17}$$

$$Y_{0\epsilon}^{ab} = \begin{pmatrix} Y_{0\epsilon}^{11} & \frac{c_2 c_f}{2r^2 t_\theta} + \frac{c_4 c_f}{2r^4 t_\theta}(r^2 f_r^2 + 3s_f^2) & 0 \\ \frac{c_2 c_f}{2r^2 t_\theta} + \frac{c_4 c_f}{2r^4 t_\theta}(r^2 f_r^2 + 3s_f^2) & Y_{0\epsilon}^{22} & 0 \\ 0 & 0 & Y_{0\epsilon}^{33} \end{pmatrix}, \tag{4.18}$$

$$Y_{1\epsilon}^{abi} = \frac{c_2}{r} c_f \begin{pmatrix} 0 & \hat{\mathbf{x}}_2^i & \hat{\mathbf{x}}_3^i \\ -\hat{\mathbf{x}}_2^i & 0 & \frac{1}{t_\theta c_f}\hat{\mathbf{x}}_3^i \\ -\hat{\mathbf{x}}_3^i & -\frac{1}{t_\theta c_f}\hat{\mathbf{x}}_3^i & 0 \end{pmatrix} + \frac{c_4}{r^2} s_f \begin{pmatrix} 4c_f f_r \hat{\mathbf{x}}_1^i & \left(\frac{3s_{2f}}{2r} + \frac{r f_r^2}{t_f}\right)\hat{\mathbf{x}}_2^i & \left(\frac{3c_{2f}}{2r} + \frac{r f_r^2}{t_f}\right)\hat{\mathbf{x}}_3^i \\ (2f_r - \frac{s_{2f}}{2r})\hat{\mathbf{x}}_2^i + \frac{2f_r}{s_\theta}\delta^{i3}\left(\frac{2s_f}{r t_\theta^2} + c_f f_r\right)\hat{\mathbf{x}}_1^i - \frac{2c_\theta s_f}{r s_\theta^2}\delta^{i3} & \cot\theta\left(\frac{s_f}{r} + \frac{r f_r^2}{s_f}\right)\hat{\mathbf{x}}_3^i \\ -\frac{s_{2f}}{2r}\hat{\mathbf{x}}_3^i & -\frac{r f_r^2}{t_\theta s_f}\hat{\mathbf{x}}_3^i & \left(\frac{s_f}{r t_\theta^2} + c_f f_r\right)\hat{\mathbf{x}}_1^i - \frac{c_\theta s_f}{r s_\theta^2}\delta^{i3} \end{pmatrix}, \tag{4.19}$$

$$Y_{2\epsilon}^{abij} = \frac{c_2}{2}\begin{pmatrix} \delta^{ij} & 0 & 0 \\ 0 & \delta^{ij} & 0 \\ 0 & 0 & \delta^{ij} \end{pmatrix} + \frac{c_4}{2}\begin{pmatrix} \frac{s_f^2}{r^2}(\delta^{ij} + \hat{\mathbf{x}}_1^i\hat{\mathbf{x}}_1^j) & \frac{s_f f_r}{r}(\hat{\mathbf{x}}_1^i\hat{\mathbf{x}}_2^j + \epsilon^{ijk}\hat{\mathbf{x}}_3^k) & \frac{s_f f_r}{r}(\hat{\mathbf{x}}_1^i\hat{\mathbf{x}}_3^j - \epsilon^{ijk}\hat{\mathbf{x}}_2^k) \\ \frac{s_f f_r}{r}(\hat{\mathbf{x}}_2^i\hat{\mathbf{x}}_1^j - \epsilon^{ijk}\hat{\mathbf{x}}_3^k) & \frac{s_f^2}{r^2}\hat{\mathbf{x}}_{!3}^i\hat{\mathbf{x}}_{!3}^j + f_r^2\hat{\mathbf{x}}_{!1}^i\hat{\mathbf{x}}_{!1}^j & \frac{s_f^2}{r^2}(\hat{\mathbf{x}}_2^i\hat{\mathbf{x}}_3^j + \epsilon^{ijk}\hat{\mathbf{x}}_1^k) \\ \frac{s_f f_r}{r}(\hat{\mathbf{x}}_3^i\hat{\mathbf{x}}_1^j + \epsilon^{ijk}\hat{\mathbf{x}}_2^k) & \frac{s_f^2}{r^2}(\hat{\mathbf{x}}_3^i\hat{\mathbf{x}}_2^j - \epsilon^{ijk}\hat{\mathbf{x}}_1^k) & \frac{s_f^2}{r^2}\hat{\mathbf{x}}_{!2}^i\hat{\mathbf{x}}_{!2}^j + f_r^2\hat{\mathbf{x}}_{!1}^i\hat{\mathbf{x}}_{!1}^j \end{pmatrix}, \tag{4.20}$$

for the quadratic N^{2}LO terms and

$$Z_0^{111} = \frac{\mu^2}{6}\cos^{s-3} f(1-\cos^2 f)^{p-3}\sin f\Big((s-1)(-3+(1+s)\sin^2 f) + (sp-1)\cos^{2s} f(-3+(sp+1)\sin^2 f) + \cos^s f(3(s(p+1)-2)+(2+s^2(1-3p))\sin^2 f)\Big) + \frac{c_6}{r^4}\sin(2f)(2-5\sin^2 f)f_r^2, \tag{4.21}$$

JHEP11(2022)092

$$Z_0^{222} = -\frac{3c_6}{r^4}\cot\theta\sin^3(f)f_r^2, \tag{4.22}$$

$$Z_0^{112} = \frac{3c_6}{4r^4}\cot\theta(3\sin(3f)-\sin f)f_r^2, \tag{4.23}$$

$$\begin{aligned} Z_0^{221} = {} & \frac{\mu^2}{2}\cos^{s-1}f(1-\cos^s f)^{p-2}(1-s+(sp-1)\cos^s f)\sin f \\ & + \frac{c_6}{r^4}\sin(2f)(\cot^2\theta-3\sin^2 f)f_r^2, \end{aligned} \tag{4.24}$$

$$Z_0^{331} = \frac{\mu^2}{2}\cos^{s-1}f(1-\cos^s f)^{p-2}(1-s+(sp-1)\cos^s f)\sin f - \frac{3c_6}{r^4}\sin^2 f\sin(2f)f_r^2, \tag{4.25}$$

$$Z_0^{332} = -\frac{3c_6}{r^4}\cot\theta\sin^3(f)f_r^2, \tag{4.26}$$

$$Z_1^{1bci} = \frac{c_6}{r^4}s_f^2 f_r \begin{pmatrix} 3(4-5s_f^2)\hat{\mathbf{x}}_1^i & 6c_f(\hat{\mathbf{x}}_2^i+\csc\theta\delta^{i3}) & 0 \\ 6c_f(\hat{\mathbf{x}}_2^i+\csc\theta\delta^{i3}) & \left(\frac{2}{t_\theta^2}-3s_f^2\right)\hat{\mathbf{x}}_1^i & 0 \\ 0 & 0 & -3s_f^2\hat{\mathbf{x}}_1^i \end{pmatrix}, \tag{4.27}$$

$$\begin{aligned} Z_1^{2bci} = {} & \frac{c_6}{r^3}s_f f_r \begin{pmatrix} 3(2-3s_f^2)f_r\hat{\mathbf{x}}_2^i & c_f\left(\frac{3s_{2f}}{2r}+\frac{4f_r}{t_\theta^2}\right)\hat{\mathbf{x}}_1^i & 0 \\ c_f\left(\frac{3s_{2f}}{2r}+\frac{4f_r}{t_\theta^2}\right)\hat{\mathbf{x}}_1^i & \left(\frac{2s_{2f}}{r}+\frac{2f_r}{t_\theta^2}-3s_f^2 f_r\right)\hat{\mathbf{x}}_2^i & 0 \\ 0 & 0 & -3s_f^2 f_r\hat{\mathbf{x}}_2^i \end{pmatrix} \\ & + \frac{2c_6}{r^3}\frac{s_{2f}f_r}{s_\theta}\begin{pmatrix} 0 & -\frac{f_r}{t_\theta} & 0 \\ -\frac{f_r}{t_\theta} & \frac{s_f}{r} & 0 \\ 0 & 0 & 0 \end{pmatrix}\delta^{i3}, \end{aligned} \tag{4.28}$$

$$\begin{aligned} Z_1^{3bci} = {} & \frac{c_6}{r^3}s_f f_r \begin{pmatrix} 3(2-3s_f^2)f_r\hat{\mathbf{x}}_3^i & \frac{2c_f f_r}{t_\theta}\hat{\mathbf{x}}_3^i & c_f\left(\frac{3s_{2f}}{2r}+\frac{2f_r}{t_\theta^2}\right)\hat{\mathbf{x}}_1^i \\ \frac{2c_f f_r}{t_\theta}\hat{\mathbf{x}}_3^i & -3s_f^2 f_r\hat{\mathbf{x}}_3^i & \left(\frac{s_{2f}}{r}+\frac{f_r}{t_\theta^2}\right)\hat{\mathbf{x}}_2^i \\ c_f\left(\frac{3s_{2f}}{2r}+\frac{2f_r}{t_\theta^2}\right)\hat{\mathbf{x}}_1^i & \left(\frac{s_{2f}}{r}+\frac{f_r}{t_\theta^2}\right)\hat{\mathbf{x}}_2^i & -3s_f^2 f_r\hat{\mathbf{x}}_3^i \end{pmatrix} \\ & + \frac{c_6}{r^3}\frac{s_{2f}f_r}{s_\theta}\begin{pmatrix} 0 & 0 & -\frac{f_r}{t_\theta} \\ 0 & 0 & \frac{s_f}{r} \\ -\frac{f_r}{t_\theta} & \frac{s_f}{r} & 0 \end{pmatrix}\delta^{i3}, \end{aligned} \tag{4.29}$$

$$Z_2^{ab1ij} = \frac{c_6}{r^2}s_{2f}\begin{pmatrix} \frac{2s_f^2}{r^2}\hat{\mathbf{x}}_1^i\hat{\mathbf{x}}_1^j & \frac{3s_f f_r}{2r}(\hat{\mathbf{x}}_1^i\hat{\mathbf{x}}_2^j+\epsilon^{ijk}\hat{\mathbf{x}}_3^k) & \frac{3s_f f_r}{2r}(\hat{\mathbf{x}}_1^i\hat{\mathbf{x}}_3^j-\epsilon^{ijk}\hat{\mathbf{x}}_2^k) \\ \frac{3s_f f_r}{2r}(\hat{\mathbf{x}}_2^i\hat{\mathbf{x}}_1^j-\epsilon^{ijk}\hat{\mathbf{x}}_3^k) & f_r^2\hat{\mathbf{x}}_2^i\hat{\mathbf{x}}_2^j & f_r^2(\hat{\mathbf{x}}_2^i\hat{\mathbf{x}}_3^j+\epsilon^{ijk}\hat{\mathbf{x}}_1^k) \\ \frac{3s_f f_r}{2r}(\hat{\mathbf{x}}_3^i\hat{\mathbf{x}}_1^j+\epsilon^{ijk}\hat{\mathbf{x}}_2^k) & f_r^2(\hat{\mathbf{x}}_3^i\hat{\mathbf{x}}_2^j-\epsilon^{ijk}\hat{\mathbf{x}}_1^k) & f_r^2\hat{\mathbf{x}}_3^i\hat{\mathbf{x}}_3^j \end{pmatrix}, \tag{4.30}$$

$$Z_2^{ab2ij} = \frac{c_6}{r^2}s_f\begin{pmatrix} \frac{2s_f^2}{r^2}(\hat{\mathbf{x}}_2^i\hat{\mathbf{x}}_1^j+s_\theta^{-1}\delta^{i3}\hat{\mathbf{x}}_1^j) & Z_2^{122ij} & Z_2^{132ij} \\ Z_2^{212ij} & \frac{s_{2f}f_r}{r}(\hat{\mathbf{x}}_2^i\hat{\mathbf{x}}_1^j-\frac{1}{2}\epsilon^{ijk}\hat{\mathbf{x}}_3^k)+\frac{2f_r^2}{t_\theta}\hat{\mathbf{x}}_2^i\hat{\mathbf{x}}_2^j & Z_2^{232ij} \\ Z_2^{312ij} & Z_2^{322ij} & 0 \end{pmatrix}, \tag{4.31}$$

$$Z_2^{122ij} = Z_2^{212ji} = \frac{2s_f f_r}{r}\hat{\mathbf{x}}_2^i\hat{\mathbf{x}}_2^j + \frac{s_f s_{2f}}{2r^2}\hat{\mathbf{x}}_1^i\hat{\mathbf{x}}_1^j + \frac{2s_f f_r}{rt_\theta}\epsilon^{ijk}\hat{\mathbf{x}}_3^k + \frac{2s_f f_r}{rs_\theta}\delta^{i3}\hat{\mathbf{x}}_2^j, \tag{4.32}$$

JHEP11(2022)092

$$Z_2^{132ij} = Z_2^{312ji} = \frac{s_f f_r}{r}(\hat{\mathbf{x}}_2^i\hat{\mathbf{x}}_3^j + \epsilon^{ijk}\hat{\mathbf{x}}_1^k - s_\theta^{-1}\hat{\mathbf{x}}_3^i\delta^{j3} + 2s_\theta^{-1}\delta^{i3}\hat{\mathbf{x}}_3^j), \tag{4.33}$$

$$Z_2^{232ij} = Z_2^{322ji} = \frac{f_r^2}{t_\theta}(\hat{\mathbf{x}}_2^i\hat{\mathbf{x}}_3^j + \epsilon^{ijk}\hat{\mathbf{x}}_1^k) + \frac{s_{2f}f_r}{2r}(\hat{\mathbf{x}}_1^i\hat{\mathbf{x}}_3^j - \epsilon^{ijk}\hat{\mathbf{x}}_2^k), \tag{4.34}$$

$$Z_2^{ab3ij} = \frac{c_6}{r^2}s_f \begin{pmatrix} 0 & 0 & Z_2^{133ij} \\ 0 & 0 & Z_2^{233ij} \\ Z_2^{313ij} & Z_2^{323ij} & \frac{2f_r^2}{t_\theta}(\hat{\mathbf{x}}_2^i\hat{\mathbf{x}}_3^j - \frac{t_\theta}{2}\epsilon^{ijk}\hat{\mathbf{x}}_2^k) + \frac{s_{2f}f_r}{r}(\hat{\mathbf{x}}_1^i\hat{\mathbf{x}}_3^j + \frac{1}{2}\epsilon^{ijk}\hat{\mathbf{x}}_2^k) - \frac{f_r^2}{s_\theta}\epsilon^{ij3} \end{pmatrix}, \tag{4.35}$$

$$Z_2^{133ij} = Z_2^{313ji} = \frac{s_f f_r}{r}(\hat{\mathbf{x}}_2^i\hat{\mathbf{x}}_2^j + t_\theta^{-1}\epsilon^{ijk}\hat{\mathbf{x}}_3^k + s_\theta^{-1}\delta^{i3}\hat{\mathbf{x}}_2^j) + \frac{s_{2f}s_f}{2r^2}\hat{\mathbf{x}}_1^i\hat{\mathbf{x}}_1^j, \tag{4.36}$$

$$Z_2^{233ij} = Z_2^{323ji} = \frac{f_r^2}{t_\theta}\hat{\mathbf{x}}_2^i\hat{\mathbf{x}}_2^j + \frac{s_{2f}f_r}{2r}(\hat{\mathbf{x}}_1^i\hat{\mathbf{x}}_2^j + \epsilon^{ijk}\hat{\mathbf{x}}_3^k), \tag{4.37}$$

$$Z_3^{112ijk} = \frac{4c_6}{r^3}s_f^3\left(\hat{\mathbf{x}}_1^i\epsilon^{jkl}\hat{\mathbf{x}}_3^l + \frac{1}{2}\epsilon^{ijl}\hat{\mathbf{x}}_3^l\hat{\mathbf{x}}_1^k\right), \tag{4.38}$$

$$Z_3^{113ijk} = \frac{4c_6}{r^3}s_f^3\left(-\hat{\mathbf{x}}_1^i\epsilon^{jkl}\hat{\mathbf{x}}_2^l - \frac{1}{2}\epsilon^{ijl}\hat{\mathbf{x}}_2^l\hat{\mathbf{x}}_1^k\right), \tag{4.39}$$

$$Z_3^{221ijk} = \frac{4c_6}{r^2}s_f^2 f_r\left(-\hat{\mathbf{x}}_2^i\epsilon^{jkl}\hat{\mathbf{x}}_3^l - \frac{1}{2}\epsilon^{ijl}\hat{\mathbf{x}}_3^l\hat{\mathbf{x}}_2^k\right), \tag{4.40}$$

$$Z_3^{123ijk} = \frac{4c_6}{r^2}s_f^2 f_r\left(\hat{\mathbf{x}}_1^i\epsilon^{jkl}\hat{\mathbf{x}}_1^l + \frac{1}{2}\epsilon^{ijl}\hat{\mathbf{x}}_1^l\hat{\mathbf{x}}_1^k + \epsilon^{ijl}\hat{\mathbf{x}}_3^l\hat{\mathbf{x}}_3^k + \frac{1}{2}\hat{\mathbf{x}}_3^i\epsilon^{jkl}\hat{\mathbf{x}}_3^l\right), \tag{4.41}$$

$$Z_3^{223ijk} = \frac{4c_6}{r}s_f f_r^2\left(\hat{\mathbf{x}}_2^i\epsilon^{jkl}\hat{\mathbf{x}}_1^l + \frac{1}{2}\epsilon^{ijl}\hat{\mathbf{x}}_1^l\hat{\mathbf{x}}_2^k\right), \tag{4.42}$$

$$Z_3^{332ijk} = \frac{4c_6}{r}s_f f_r^2\left(-\hat{\mathbf{x}}_3^i\epsilon^{jkl}\hat{\mathbf{x}}_1^l - \frac{1}{2}\epsilon^{ijl}\hat{\mathbf{x}}_1^l\hat{\mathbf{x}}_3^k\right), \tag{4.43}$$

for the cubic N^{2}LO terms.

The equations of motion for the general fluctuations in Cartesian coordinates read

$$\begin{aligned}&\partial_i\left(\Omega^b Y_1^{bai} + \epsilon\Omega^b Y_{1\epsilon}^{bai} + 2Y_2^{abij}\partial_j\Omega^b + 2\epsilon Y_{2\epsilon}^{abij}\partial_j\Omega^b\right)\\ &\quad - 2Y_0^{ab}\Omega^b - 2\epsilon Y_{0\epsilon}^{ab}\Omega^b - Y_1^{abi}\partial_i\Omega^b - \epsilon Y_{1\epsilon}^{abi}\partial_i\Omega^b = \epsilon X_{0\epsilon}^a - \epsilon\partial_i(X_{1\epsilon}^a\hat{\mathbf{x}}_a^i),\end{aligned} \tag{4.44}$$

(a not summed over). We have used the short-hand notation for the trigonometric functions

$$s_\theta = \sin\theta, \quad s_f = \sin f, \quad c_\theta = \cos\theta, \quad c_f = \cos f, \quad t_\theta = \tan\theta, \tag{4.45}$$

and so on, and we have used the following short-hand index summation rule

$$\hat{\mathbf{x}}_{!1}^i\hat{\mathbf{x}}_{!1}^j := \sum_{a\neq 1}\hat{\mathbf{x}}_a^i\hat{\mathbf{x}}_a^j = \delta^{ij} - \hat{\mathbf{x}}_1^i\hat{\mathbf{x}}_1^j, \tag{4.46}$$

and similarly for other excluded directions.

4.2 Spherical symmetry

We will now show that if we restrict to the spherically symmetric $B = 1$ Skyrmion and impose $\delta f = \delta f(r)$, the fluctuations $\delta\theta$ and $\delta\varphi$ decouple and are solved by their trivial solution.

JHEP11(2022)092

First we notice that there are, seemingly, source terms for the fluctuation field $\delta\theta$ in eqs. (4.7) and (4.8). However, using the identity

$$\partial_i X = \hat{\mathbf{x}}_1^i \partial_r X + \frac{1}{r}\hat{\mathbf{x}}_2^i \partial_\theta X + \frac{1}{r\sin\theta}\hat{\mathbf{x}}_3^i \partial_\varphi X, \tag{4.47}$$

the linear terms in the energy density (4.3) for the fluctuations $\delta\theta$ and $\delta\varphi$ read

$$\epsilon \sin f \left(\frac{c_2}{r^2} + \frac{c_4}{r^4}\sin^2 f + \frac{c_4}{r^2} f_r^2\right)(\cot\theta\delta\theta + \partial_\theta\delta\theta + \partial_\varphi\delta\varphi)\,. \tag{4.48}$$

Now including the integration measure, we have

$$\begin{aligned}
&\epsilon \int \mathrm{d}r\mathrm{d}\theta\delta\varphi \sin f \left(c_2 + \frac{c_4}{r^2}\sin^2 f + c_4 f_r^2\right)(\cos\theta\delta\theta + \sin\theta\partial_\theta\delta\theta + \sin\theta\partial_\varphi\delta\varphi) \\
&= \epsilon \int \mathrm{d}r\mathrm{d}\theta\delta\varphi\, \partial_\theta \left[\sin f \left(c_2 + \frac{c_4}{r^2}\sin^2 f + c_4 f_r^2\right)\sin\theta\delta\theta\right] \\
&\quad + \epsilon \int \mathrm{d}r\mathrm{d}\theta\delta\varphi\, \partial_\varphi \left[\sin\theta \sin f \left(c_2 + \frac{c_4}{r^2}\sin^2 f + c_4 f_r^2\right)\delta\varphi\right],
\end{aligned} \tag{4.49}$$

which are clearly total derivatives and hence do no contribute to the equations of motion for the fluctuation fields. In particular, this means that the sources, i.e. the right-hand side of the equation of motion (4.44) take the form

$$\epsilon \begin{pmatrix} * \\ 0 \\ 0 \end{pmatrix}, \tag{4.50}$$

thus are only turning on the fluctuation $\delta f = \Omega^1$.

Next, we will show that only the non-radial derivatives of δf turn on the fluctuations $\delta\theta$ and $\delta\varphi$. Starting with the non-derivative terms in the equations of motion (4.44), we observe that

$$\partial_i (Y_1^i)^{\mathrm{T}} - 2Y_0 = \begin{pmatrix} * & * & 0 \\ 0 & * & 0 \\ 0 & 0 & * \end{pmatrix}, \qquad \partial_i (Y_{1\epsilon}^i)^{\mathrm{T}} - 2Y_{0\epsilon} = \begin{pmatrix} * & * & 0 \\ 0 & * & 0 \\ 0 & 0 & * \end{pmatrix}, \tag{4.51}$$

where we treat the tensors as matrices in ab: $a = 1, 2, 3$ being the row and the equation index and $b = 1, 2, 3$ being the column and field index. It is thus clear — at this stage — that a nonvanishing $\delta\theta$ affects the equation of motion for δf, but a nonvanishing δf does not affect the equations of motion for $\delta\theta$ and $\delta\varphi$: it does not act as a source for the latter fluctuation fields.

JHEP11(2022)092

Considering now the one-derivative terms of the equations of motion, we find

$$\left[(Y_1^i)^{\mathrm{T}} - Y_1^i + 2\partial_j Y_2^{ji}\right]\hat{\mathbf{x}}_1^i = \begin{pmatrix} * & * & 0 \\ 0 & * & 0 \\ 0 & 0 & * \end{pmatrix}, \qquad \left[(Y_{1\epsilon}^i)^{\mathrm{T}} - Y_{1\epsilon}^i + 2\partial_j Y_{2\epsilon}^{ji}\right]\hat{\mathbf{x}}_1^i = \begin{pmatrix} * & * & 0 \\ 0 & * & 0 \\ 0 & 0 & * \end{pmatrix},$$

$$\left[(Y_1^i)^{\mathrm{T}} - Y_1^i + 2\partial_j Y_2^{ji}\right]\hat{\mathbf{x}}_2^i = \begin{pmatrix} 0 & * & 0 \\ * & * & 0 \\ 0 & 0 & * \end{pmatrix}, \qquad \left[(Y_{1\epsilon}^i)^{\mathrm{T}} - Y_{1\epsilon}^i + 2\partial_j Y_{2\epsilon}^{ji}\right]\hat{\mathbf{x}}_2^i = \begin{pmatrix} 0 & * & 0 \\ * & * & 0 \\ 0 & 0 & * \end{pmatrix},$$

$$\left[(Y_1^i)^{\mathrm{T}} - Y_1^i + 2\partial_j Y_2^{ji}\right]\hat{\mathbf{x}}_3^i = \begin{pmatrix} 0 & 0 & * \\ 0 & 0 & 0 \\ * & * & 0 \end{pmatrix}, \qquad \left[(Y_{1\epsilon}^i)^{\mathrm{T}} - Y_{1\epsilon}^i + 2\partial_j Y_{2\epsilon}^{ji}\right]\hat{\mathbf{x}}_3^i = \begin{pmatrix} 0 & 0 & * \\ 0 & 0 & * \\ * & * & 0 \end{pmatrix}, \tag{4.52}$$

from which we can see that a nonvanishing radial derivative of the fluctuation $\partial_r \delta f$ does not turn on the fluctuations $\delta\theta$ and $\delta\varphi$ (see the first line), whereas a nonvanishing $\partial_\theta \delta f$ acts as a source for $\delta\theta$ (see the second line) and a nonvanishing $\partial_\varphi \delta f$ acts as a source for $\delta\varphi$, recalling the identity (4.47) (see the third line).

Finally, we need to consider the double-derivatives of the fluctuation fields in the equations of motion and we find

$$(Y_2^{ij} + Y_2^{ji})\hat{\mathbf{x}}_k^i \hat{\mathbf{x}}_l^j \propto \delta^{ka}\delta^{lb} + \delta^{kb}\delta^{la}, \qquad (Y_{2\epsilon}^{ij} + Y_{2\epsilon}^{ji})\hat{\mathbf{x}}_k^i \hat{\mathbf{x}}_l^j \propto \delta^{kl}\delta^{ab} + \delta^{ka}\delta^{lb} + \delta^{kb}\delta^{la}, \tag{4.53}$$

(distinguishing only vanishing and nonvanishing elements of the tensor and with ab being the matrix indices) and hence it is clear again that the only sources for the fluctuations $\delta\theta$ and $\delta\varphi$ are $\partial_r\partial_\theta\delta f$ and $\partial_r\partial_\varphi\delta f$.

This completes the proof that $\delta f = \delta f(r)$ does not turn on the fluctuations $\delta\theta$ or $\delta\varphi$ and their equations of motion are homogeneous and satisfied by $\delta\theta = \delta\varphi = 0$, which is compatible with their boundary conditions at spatial infinity. Hence, without a nonspherical fluctuation field δf, the angular fluctuation fields remain turned off.

4.3 Boundary conditions

The equation of motion (4.44) must be accompanied by suitable boundary conditions: the cusp condition at the boundary of the $B = 1$ compacton, the fluctuations must vanish at spatial infinity and finally, we will solve the problem of binding energies by performing a mirror trick similar to the problem in two dimensions [23], see figure 4.

A problem is that the best coordinates for imposing the cusp condition on the boundary of the compacton are the spherical coordinates with origin O, whereas the best coordinates for imposing the gluing conditions at $x = 0$ are Cartesian coordinates. Here, we will utilize the fact that we are only solving the linearized equation of motion (4.44) and hence, we can find the solution using the superposition of two solutions:

$$\delta f = \delta f^{\mathrm{rad}} + \delta f^{\mathrm{glue}}, \tag{4.54}$$

which is the sum of the radial fluctuation of section 3.4, δf^{rad}, that solves the cusp condition on the boundary of the compacton and a new fluctuation field δf^{glue} that is only subject to the gluing condition as well as the boundary condition at spatial infinity.

JHEP11(2022)092

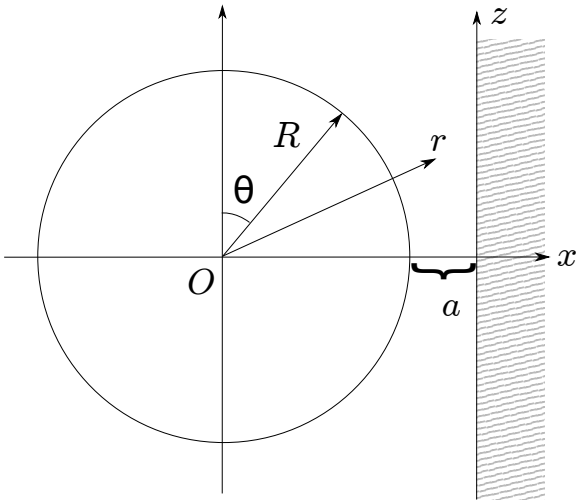

Figure 4. Setup for computation of the binding energy between two $B = 1$ Skyrmions using the mirror trick and certain gluing conditions at $x = 0$ and the $B = 1$ Skyrmion is placed at $x = -R-a$. The figure is shown at $y = \varphi = 0$.

The solution for the $B = 1$ Skyrmion that obeys the cusp condition δf^{rad} is exactly the fluctuation found in section 3.4; the new fluctuation field subject to the gluing conditions can thus be calculated in Cartesian coordinates, which is why we have written the energy of section 4.1 in Cartesian coordinates. Notice that the field δf^{glue} experiences a smooth background, since the cusp condition and the termination of the BPS solution on the compacton boundary add up to a smooth total field. We will now discuss the gluing condition in more details next.

4.4 Gluing condition

We will assume that the two $B = 1$ Skyrmions should be placed in their attractive channel, which is dictated by viewing the Skyrmions as triplets of dipoles, which by the kinetic term provides and attractive channel [42][3]. The gluing conditions for the attractive channel of two $B = 1$ Skyrmions are

$$\begin{pmatrix} \partial_x \Phi^0 \\ \partial_x \Phi^1 \\ \Phi^2 \\ \partial_x \Phi^2 \end{pmatrix} = 0, \tag{4.55}$$

where 3 conditions are Neumann and one is Dirichlet, which is necessary for computing the gluing with Skyrmions in the attractive channel (e.g. all Neumann condition would lead to a Skyrmion-anti-Skyrmion pair). In order to impose the correct boundary conditions on

[3]See also ref. [43] for an explicit numerical computation of the interaction potential.

JHEP11(2022)092

the fluctuation fields, we first write out the total field

$$\begin{aligned}\Phi &= \Phi + \delta\Phi \\ &= \Phi + \Phi_r \delta f + \Phi_\theta \delta\theta + \Phi_\varphi \delta\varphi - \frac{1}{2}\Phi(\delta f^2 + \delta\theta^2 + \delta\varphi^2).\end{aligned} \tag{4.56}$$

Since the gluing condition should be applied outside the domain of the compacton, we need to set $f = 0$ of the background solution, for which the total field reads

$$\Phi = \begin{pmatrix}1\\0\\0\\0\end{pmatrix}\left(1 - \frac{\delta f^2}{2} - \frac{\delta\theta^2}{2} - \frac{\delta\varphi^2}{2}\right) + \begin{pmatrix}0\\\sin\theta\cos\varphi\\\sin\theta\sin\varphi\\\cos\theta\end{pmatrix}\delta f + \begin{pmatrix}0\\\cos\theta\cos\varphi\\\cos\theta\sin\varphi\\-\sin\theta\end{pmatrix}\delta\theta + \begin{pmatrix}0\\-\sin\varphi\\\cos\varphi\\0\end{pmatrix}\delta\varphi. \tag{4.57}$$

Using the identity (4.47), we obtain the following gluing conditions for the fluctuation fields

$$\delta f \delta f_x + \delta\theta\delta\theta_x + \delta\varphi\delta\varphi_x = 0, \tag{4.58}$$

$$\sin\theta\sin\varphi\delta f + \cos\theta\sin\varphi\delta\theta + \cos\varphi\delta\varphi = 0, \tag{4.59}$$

$$\frac{1}{r}\cos\theta\cos\varphi(\cos\theta\delta f - \sin\theta\delta\theta) + \sin\theta\delta f_x + \cos\theta\delta\theta_x - \tan\varphi\delta\varphi_x = 0, \tag{4.60}$$

$$\frac{1}{r}\cos\varphi(\sin\theta\delta f + \cos\theta\delta\theta) - \delta f_x + \tan\theta\delta\theta_x = 0. \tag{4.61}$$

Since this is a complicated mixture of a nonlinear boundary condition and a Robin-type boundary condition on the fluctuation fields, we will solve the linear Robin-part of the boundary condition and verify a posteriori that the quadratic part is approximately satisfied. Using the discrete x-derivative to order h_x^2 with h_x being the lattice spacing, the solution reads

$$\begin{aligned}\delta f_0^{\text{glue}} &= \frac{3r^2(\cos^2\theta + \sin^2\theta\cos^2\varphi)}{4h_x^2\cos^2\theta\cos^4\varphi + 9r^2}(4\delta f_{-1}^{\text{glue}} - \delta f_{-2}^{\text{glue}}) \\ &\quad + \frac{r\cos\theta(2h_x\cos^3\varphi - 3r\sin\theta\sin^2\varphi)}{4h_x^2\cos^2\theta\cos^4\varphi + 9r^2}(4\delta\theta_{-1} - \delta\theta_{-2}) \\ &\quad - \frac{r\sin(2\varphi)(2h_x\cos^2\theta\cos\varphi + 3r\sin\theta)}{2(4h_x^2\cos^2\theta\cos^4\varphi + 9r^2)}(4\delta\varphi_{-1} - \delta\varphi_{-2}) \\ &\quad + \frac{4h_x^2\cos^2\theta\cos^4\varphi + 9r^2\sin^2\theta\sin^2\varphi}{4h_x^2\cos^2\theta\cos^4\varphi + 9r^2}\delta f^{\text{rad}} \\ &\quad + \frac{6h_x r^2\sin\theta\cos\varphi(\cos^2\theta + \sin^2\theta\cos^2\varphi)}{4h_x^2\cos^2\theta\cos^4\varphi + 9r^2}\delta f_r^{\text{rad}},\end{aligned} \tag{4.62}$$

$$\begin{aligned}\delta\theta_0 &= \frac{r(2h_x\cos^3\varphi + 3r\sin\theta\sin^2\varphi)}{4h_x^2\cos\theta\cos^4\varphi + 9r^2}(4\delta f_{-1}^{\text{glue}} - \delta f_{-2}^{\text{glue}}) \\ &\quad - \frac{3r^2(2h_x\cos^4\theta\cos^3\varphi + 3r\sin\theta\cos^2\varphi + 2h_x\cos^2\theta\sin^2\theta\cos\varphi + 3r\sin^3\theta\sin^2\varphi)}{(4h_x^2\cos^2\theta\cos^4\varphi + 9r^2)(2h_x\cos^2\theta + 3r\sin\theta)} \\ &\quad \times (4\delta\theta_{-1} - \delta\theta_{-2})\end{aligned}$$

JHEP11(2022)092

$$
\begin{aligned}
&+\frac{r\sin(2\varphi)(12h_x r\cos(2\theta)\cos\theta\cos\varphi-\sin(2\theta)(4h_x^2\cos^2\theta\cos^2\varphi-9r^2)}{4(4h_x^2\cos^2\theta\cos^4\varphi+9r^2)(2h_x\cos^2\theta\cos\varphi+3r\sin\theta)}\\
&\quad\times(4\delta\varphi_{-1}-\delta\varphi_{-2})\\
&+\frac{3r\cos\theta(4h_x^2c_\theta^2c_\varphi^4+6h_xrc_\theta^2s_\theta c_\varphi+9r^2s_\theta^2s_\varphi^2+6h_xrs_\theta^3c_\varphi^3)}{(4h_x^2\cos^2\theta\cos^4\varphi+9r^2)(2h_x\cos^2\theta\cos\varphi+3r\sin\theta)}\delta f^{\mathrm{rad}}\\
&-\frac{h_xr\sin(2\theta)\cos\varphi(2h_x\cos^4\varphi+3r\sin\theta\sin^2\varphi)}{4h_x^2\cos^2\theta\cos^4\varphi+9r^2}\delta f_r^{\mathrm{rad}},
\end{aligned}
\tag{4.63}
$$

$$
\begin{aligned}
\delta\varphi_0=&-\frac{r\sin(2\varphi)(2h_x\cos^2\theta\cos\varphi-3r\sin\theta)}{2(4h_x^2\cos^2\theta\cos^4\varphi+9r^2)}(4\delta f_{-1}^{\mathrm{glue}}-\delta f_{-2}^{\mathrm{glue}})\\
&-\frac{2r\cos\theta\sin(2\varphi)(3r+2h_x\sin\theta\cos\varphi)}{3(h_x^2+12r^2)+h^2(3\cos(2\theta)+2\cos^2\theta(4\cos(2\varphi)+\cos(4\varphi)))}(4\delta\theta_{-1}-\delta\theta_{-2})\\
&+\frac{3r^2\sin^2\varphi}{4h_x^2\cos^2\theta\cos^4\varphi+9r^2}(4\delta\varphi_{-1}-\delta\varphi_{-2})\\
&+\frac{6r\sin(2\varphi)(3r\sin\theta-2h_x\cos^2\theta\cos\varphi)}{3(h_X^2+12r^2)+h_x^2(3\cos(2\theta)+2\cos^2\theta(4\cos(2\varphi)+\cos(4\varphi)))}\delta f^{\mathrm{rad}}\\
&+\frac{4h_xr\cos\varphi\sin(2\varphi)\sin\theta(2h_x\cos^2\theta\cos\varphi-3r\sin\theta)}{3(h_x^2+12r^2)+h_x^2(3\cos(2\theta)+2\cos^2\theta(4\cos(2\varphi)+\cos(4\varphi)))}\delta f_r^{\mathrm{rad}}.
\end{aligned}
\tag{4.64}
$$

It is simple to check that the gluing condition is regular for $3r > 2h_x$, which is always true for the gluing condition since $r > R$, where $R = 1 \gg h_x$ in numerical calculations. The subscripts on the fluctuation fields correspond to lattice indices in the x-direction, i.e. $\delta\theta_0$ corresponds to $\delta\theta(x=0)$, $\delta\theta_{-1} = \delta\theta(x=-h_x)$ and $\delta\theta_{-2} = \delta\theta(x=-2h_x)$ and similarly for the other fluctuation fields. The coordinate system for the spherical polar coordinates is

$$
x + R + a + \mathrm{i}y = r\sin\theta e^{\mathrm{i}\varphi}, \qquad z = r\cos\theta. \tag{4.65}
$$

With the gluing conditions in hand, we are now ready to perform numerical computations of the binding energies.

4.5 Numerical results

We will now compute the binding energies numerically within the semianalytic ϵ-expansion up to N^{2}LO, i.e. $\mathcal{O}(\epsilon^3)$. We choose the potential $(s,p) = (1,2)$ which corresponds to $(1-\cos f)^2$ because this potential allows for the spherically symmetric Skyrmion being stable within the axially symmetric Ansatz for $c_2 = 1$ and $c_4 = 8$ (or generically any $c_4 \gg c_2R^2$). We further fix the parameters of the numerical calculation by setting $c_6 = \frac{1}{2}$ and $\mu = 1$, which yields a compacton radius, $R = (3\pi)^{\frac{1}{3}}$. Now, in order for the cusp condition to be sufficient for the ϵ-expansion scheme to capture the true Skyrmion solution, we need $m_\pi \gg 1$ and chose $m_\pi = 3$ as in section 3.4.

We will now solve the coupled PDEs (4.44) with the cusp condition taken into account by means of splitting the field (valid for the linearized equation) (4.54), vanishing boundary conditions for the fluctuations at infinity and finally the gluing conditions (4.62)–(4.64) at $x = 0$ (i.e. midway between the two spherical $B = 1$ compactons), see figure 4. The results are shown in figures 5 and 6 for $\epsilon = 0.01$ and $\epsilon = 0.0428$, respectively. The top row of each

JHEP11(2022)092

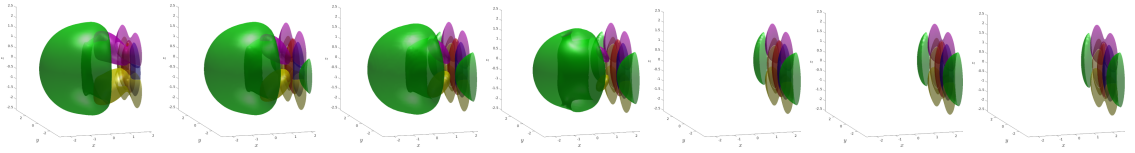

(a)

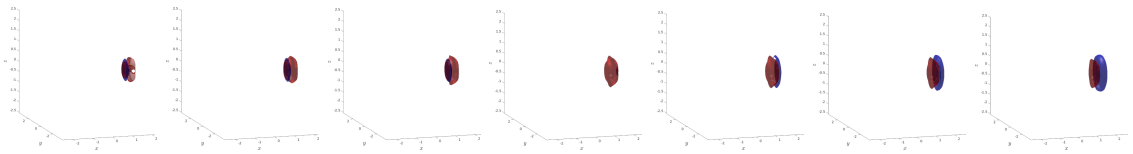

(b)

Figure 5. Numerical solution for the fluctuation fields δf^{glue}, $\delta\theta$ and $\delta\varphi$ for two $B = 1$ Skyrmions (showing only the left-hand side of the bound state) for $\epsilon = 0.01$ and separation distances $2a = (0, 1, 2, 3, 4, 5, 6)2h_x$, with $h_x \simeq 0.094$. (a) shows the field solutions with constant isosurfaces at $\frac{1}{4}$ of their respective maximal values, where the column corresponds to the separation distance. (b) shows the corresponding NLO (red) and N^{2}LO (blue) perturbation energies at $\frac{1}{4}$ of their respective minima (notice that their contributions are negative). The color coding of (a) is that positive δf^{glue} is shown with red, negative δf^{glue} with green, positive $\delta\theta$ with yellow, negative $\delta\theta$ with magenta, positive $\delta\varphi$ with blue and negative $\delta\varphi$ with orange isosurfaces. In this figure $c_2 = 1$, $c_4 = 8$, $c_6 = \frac{1}{2}$, $\mu = 1$, $m_\pi = 3$, $R = (3\pi)^{\frac{1}{3}}$ and $(s, p) = (1, 2)$.

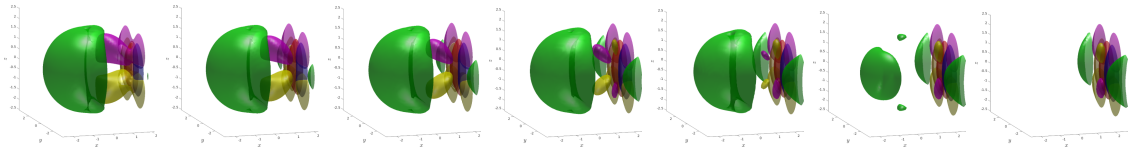

(a)

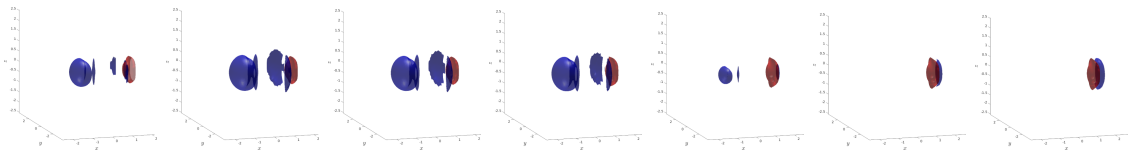

(b)

Figure 6. Numerical solution for the fluctuation fields δf^{glue}, $\delta\theta$ and $\delta\varphi$ for two $B = 1$ Skyrmions (showing only the left-hand side of the bound state) for $\epsilon = 0.0428$ and separation distances $2a = (0, 1, 2, 3, 4, 5, 6)2h_x$, with $h_x \simeq 0.094$. For further details, see the caption of figure 5.

figure shows the isosurfaces of the fluctuation fields δf^{glue}, $\delta\theta$ and $\delta\varphi$ at positive (negative) quarter-maximum (-minimum) levelsets with red, yellow and blue (green, magenta and orange), respectively. For large separation distances (right-most panels) the fluctuations are localized at the gluing boundary ($x = 0$), whereas for small or vanishing separation distances (left-most panels) the fluctuation fields are turned on throughout the compacton volume. In particular, δf makes a shallow but negative shell near the compacton border, whereas $\delta\theta$ becomes a dipole with a positive and negative blob induced in the compacton volume for small separation distances ($2a \lesssim 1$). The bottom row of the figures shows the isosurfaces of negative energy density at a quarter of the minimum value for the NLO and

JHEP11(2022)092

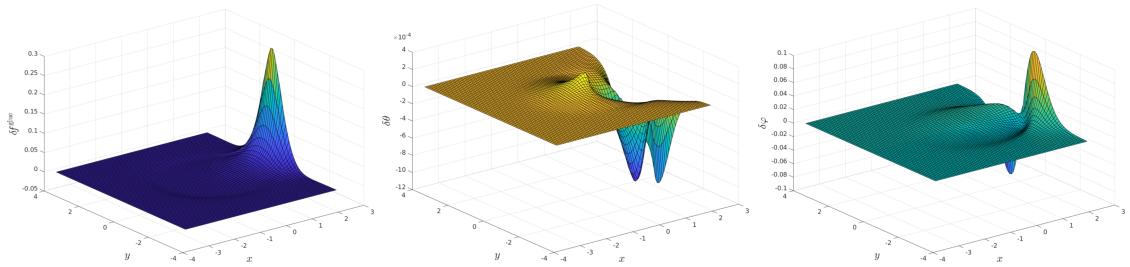

Figure 7. Numerical solution for the fluctuation fields δf^{glue} $\delta\theta$ and $\delta\varphi$ for the left half of a bound state of two $B = 1$ Skyrmions for $\epsilon = 0.01$ and vanishing separation distance $2a \simeq 0$ in the (x, y)-plane at $z = 0$.

N^{2}LO contributions to the energy from the fluctuation fields δf^{glue}, $\delta\theta$, and $\delta\varphi$ with red and blue colors, respectively. The NLO energy contribution is dominant and is responsible for the binding of the two $B = 1$ Skyrmions and is seen to be localized near the gluing boundary ($x = 0$). Figure 7 shows the fluctuation fields in the (x, y)-plane at $z = 0$ for the case of vanishing separation distance $2a \simeq 0$. The nontrivial behavior of the fluctuation fields is only induced by the gluing conditions at $x = 0$ (right-most part of each panel), but spreads a small perturbation throughout the compacton volume.

We are now ready to compute the N^{2}LO energies for the bound state of two $B = 1$ compactons using the energy (4.3) with the fluctuation fields δf^{glue}, $\delta\theta$ and $\delta\varphi$ defined in eq. (4.1). We have already placed the two $B = 1$ Skyrmions in the attractive channel by means of the Dirichlet boundary condition on Φ^2 in eq. (4.55). We furthermore know that at large separation distances, the attractive force between the two $B = 1$ Skyrmions is exponentially suppressed (due to the pion mass term), so the minimum of the energy must be at a finite separation. In the small $\epsilon \ll 1$ or near-BPS limit, we expect that the minimum of the energy of the bound state of two compactons occurs at zero separation, as was confirmed both semi-analytically within the ϵ-expansion scheme as well as numerically for baby-Skyrmions (compactons) in ref. [23]. In order to confirm that this is also the case for $B = 1$ compacton (Skyrmions) in the case of our model choice, we compute the N^{2}LO energies at different separations $2a$. The result is shown in figure 8 and establishes numerically that the minimum of the N^{2}LO energy occurs at vanishing separation of the compactons (i.e. $2a = 0$) for all presented values of ϵ, i.e. $\epsilon = 0.01, 0.0207, 0.0428, 0.0886$. The figure also shows the geometric binding energy, which is simply computed by cutting off the tail contribution to the N^{2}LO energy at $x = 0$ (so as not to over count the two tails of the two compactons). It is observed that about half of the binding energy is actually geometric for the presented range of ϵ.

The N^{2}LO energy is shown in figure 9 as a function of ϵ for vanishing separation distance ($2a = 0$). The N^{2}LO energy is below the LO energy as expected and is above the energy bound (A.8) as it must be.

We can now extract the binding energy for the two $B = 1$ Skyrmions (compactons) as a function of ϵ by comparing the N^{2}LO energies with those for infinite separations. The result is shown in figure 10. A polynomial fit to the classical binding energies in percent

JHEP11(2022)092

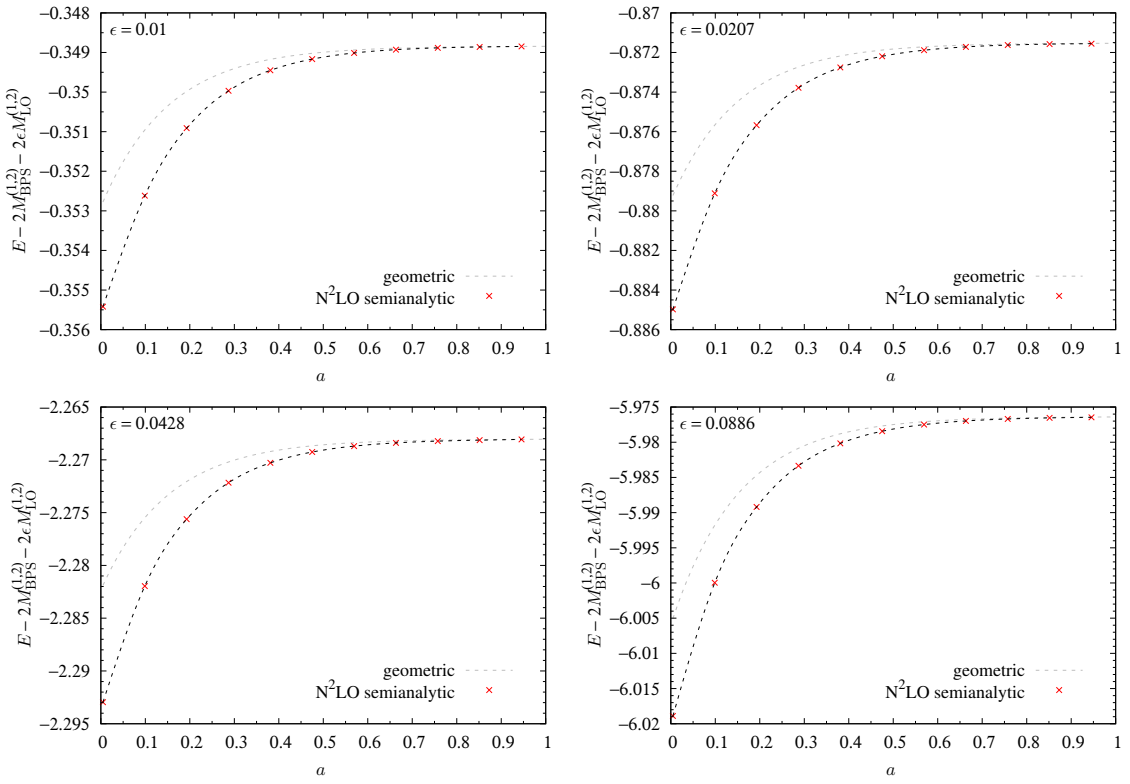

Figure 8. The N^{2}LO corrections to the energy for two $B = 1$ Skyrmions with separation distance $2a$ and $\epsilon = 0.01, 0.0207, 0.0428, 0.0886$. Asymptotically, i.e. for large values of a, the N^{2}LO corrections to the energy become exactly two times those of section 3.4. When a tends to zero, the binding energy increases monotonically with a maximum at $a = 0$, for all values of the perturbation parameter ϵ. A geometric effect of the binding energy lies simply in part of the tail energy of the $B = 1$ solutions are cut at the mirror surface $x = 0$ so as not to over count the $B = 1$ energies. This reduction of the energy is displayed as geometric with a gray dashed line. The numerical computations are always slightly below the geometric corrections. In this figure $c_2 = 1$, $c_4 = 8$, $c_6 = \frac{1}{2}$, $\mu = 1$, $m_\pi = 3$, $R = (3\pi)^{\frac{1}{3}}$ and $(s, p) = (1, 2)$.

yields

$$E^{\text{binding, deuteron}} \simeq 1.605\epsilon - 29.56\epsilon^2 + 200.8\epsilon^3. \tag{4.66}$$

Notice that this fit contains a linear term in ϵ, which is expected to come from nonanalytic behavior of the solution to the fluctuation fields. Unfortunately, the model as calibrated and chosen in order to make the cusp condition work, the spherical compactons being stable and the tails to be rapidly decaying, does not provide quite the phenomenological binding energy of the deuteron of 0.118% [44] for the range of ϵ explored. Clearly this is a crude comparison, we are not considering here quantum corrections due to the spin, iso-spin rotation, iso-spin breaking, together with the addition of the electric Coulomb interaction, which should be included in the phenomenological nuclear energies. It can furthermore be seen from the figure, that the binding energy tends to a plateau instead continuing its increase, which we interpret as loss of precision (validity) of the ϵ-expansion

JHEP11(2022)092

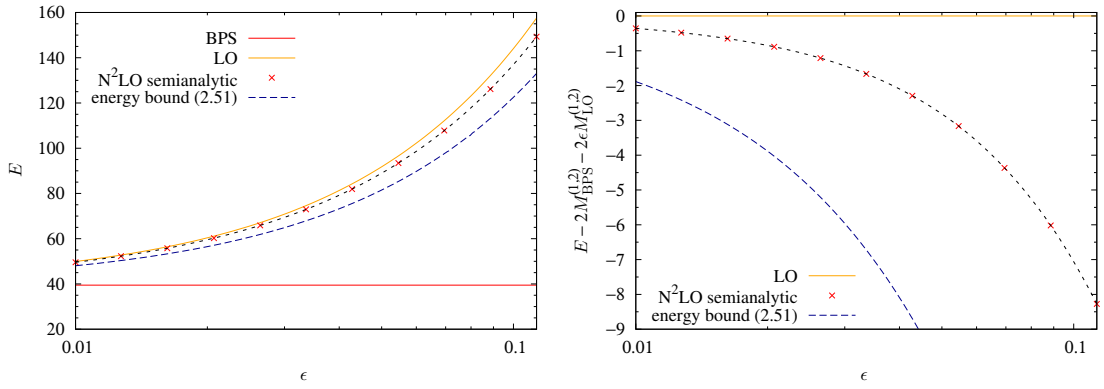

(a) (b)

Figure 9. The (a) energy and (b) N^{2}LO correction to the energy for two $B = 1$ Skyrmions with separation distance $2a = 0$ (they touch in one point) as a function of ϵ. The BPS energy is shown with a red solid line, the LO correction is shown with an orange solid line and the numerically computed N^{2}LO corrections are shown with red crosses (linked with black dashed lines for ease of reading the figure). The energy bound (A.8) is shown with a blue-dashed line. In this figure $c_2 = 1$, $c_4 = 8$, $c_6 = \frac{1}{2}$, $\mu = 1$, $m_\pi = 3$, $R = (3\pi)^{\frac{1}{3}}$ and $(s, p) = (1, 2)$.

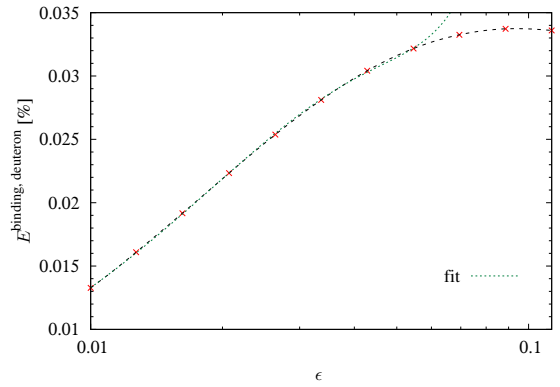

(a)

Figure 10. The binding energy per nucleon in percent for two $B = 1$ Skyrmions, i.e. the N^{2}LO energy at $a = \infty$ minus that at $a = 0$, as a function of ϵ. The physical binding energy of deuteron per nucleon for comparison is 0.118% [44]. In this figure $c_2 = 1$, $c_4 = 8$, $c_6 = \frac{1}{2}$, $\mu = 1$, $m_\pi = 3$, $R = (3\pi)^{\frac{1}{3}}$ and $(s, p) = (1, 2)$.

scheme. This is most likely because $c_4 = 8$ and hence $\epsilon \simeq 0.1129$ yields a Skyrme term coefficient of $\epsilon c_4 \sim 0.9$ which is no longer perturbative. Recall that $c_4 \gg c_2 R^2$ is needed for the spherical compacton to be a stable minimum of the energy functional. If this condition is not satisfied, the two compactons will merge and form a torus, as is well known in the standard Skyrme model [45–47].

JHEP11(2022)092

5 Physical units

It is instructive and straightforward to reinstate physical units in the model. Energies and lengths are measured in units of [48–50]

$$[\text{mass}] = \frac{F_\pi}{2\epsilon\sqrt{c_2 c_4}e}, \qquad [\text{length}] = \frac{2}{F_\pi e}\sqrt{\frac{c_2}{c_4}}, \tag{5.1}$$

respectively and the calibration of the model is readily performed by

$$F_\pi = 2\sqrt{\frac{\epsilon c_2 M_N R}{M R_N}}, \qquad e = \sqrt{\frac{MR}{\epsilon c_4 M_N R_N}}, \tag{5.2}$$

where M and R are the N^{2}LO mass and radius R of the compactons in dimensionless units, whereas M_N and R_N are the mass and radius of the nucleon in MeV. e is known as the Skyrme coupling constant and should not be confused with the charge of the electron. The physical pion mass in MeV is then given by

$$\tilde{m}_\pi = \frac{m_\pi F_\pi e}{c_2}\sqrt{\frac{c_4}{2}}, \tag{5.3}$$

the BPS potential mass in MeV is

$$\tilde{\mu} = \frac{\mu F_\pi e}{c_2}\sqrt{\frac{c_4}{2\epsilon}}, \tag{5.4}$$

and finally the coefficient of the sextic term in MeV^{-2} is

$$\tilde{c}_6 = \frac{4c_2 c_6}{\epsilon c_4^4 e^4 F_\pi^2}. \tag{5.5}$$

The calibration and coupling constants are shown in figure 11 and $\tilde{m}_\pi \simeq 2.02\,\text{GeV}$ independent of ϵ.

A comment in store is about the large pion mass in physical units. We recall from section 3.4 that the dimensionless pion mass parameter, m_π, was chosen to be abnormally large in order for the perturbative method to capture the correct asymptotic behavior of the solution, by imposing only the cusp condition at the compacton boundary ($r = R$). Choosing the dimensionless pion mass parameter about $3-6$ times larger than a usual order-one choice, obviously has an impact on the mass in physical units (linear relation). The choice of calibrating the model using the original Skyrme model (i.e. $\mathcal{L}_2 + \mathcal{L}_4$), which in our context is a small perturbation to the BPS sector, gives a large uncertainty in the physical quantities in physical units and of course many other ways to calibrate the model could be contemplated. Nevertheless, the perturbative ϵ-expansion scheme is prone to require large pion masses to be accurate; something also often seen in lattice QCD [51].

6 Conclusion and discussion

In this paper, we have considered the Skyrme model in the near-BPS limit using the perturbative ϵ-expansion scheme developed in refs. [23, 34]. The near-BPS systems we

JHEP11(2022)092

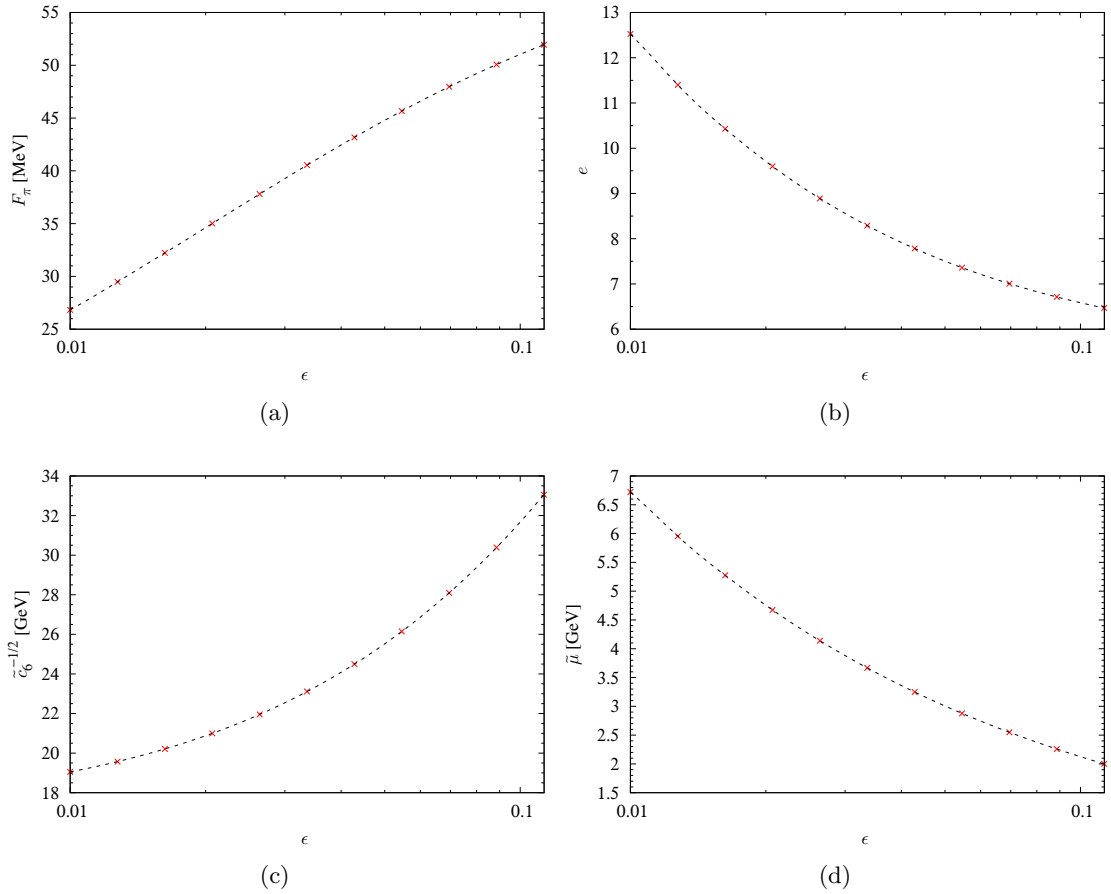

Figure 11. The Skyrme model parameters (a) F_π and (b) e in physical units (MeV) as well as the BPS sector's coupling constants (c) $\tilde{c}_6^{-\frac{1}{2}}$ and (d) $\tilde{\mu}$ in GeV. In this figure $c_2 = 1$, $c_4 = 8$, $c_6 = \frac{1}{2}$, $\mu = 1$, $m_\pi = 3$, $R = (3\pi)^{\frac{1}{3}}$ and $(s, p) = (1, 2)$.

considered consist of a BPS sector, containing a sixth-order derivative term plus a potential, and a BPS-deformation that is the original Skyrme model with massive pions. The BPS sector was chosen to give compacton-type solutions. To this end, parametrizing the BPS potential as $V_{s,p}(U) \propto (1 - (\mathrm{tr}\, U/2)^s)^p$, we select the combinations $(s, p) = (1, 2)$, $(2, 1)$, $(2, 2)$, whereas we discarded the pion mass potential $(s, p) = (1, 1)$ since we include it as a BPS-deformation.

In the ϵ-expansion scheme, the mass of the Skyrmion in the near-BPS limit is the BPS mass with corrections in powers of ϵ. The leading-order correction comes from inserting the BPS solution into the perturbation, i.e. the kinetic, the Skyrme and the pion mass terms. Before explicitly performing the calculation, we checked if all the BPS solutions lead to a finite LO energy contribution. To test this, we found a general criterion based on the behavior of the potential around the vacuum value. We have shown that, besides the pion mass potential, also the potential $(s, p) = (2, 1)$ generates a divergent LO energy and for this reason we discarded it from our study.

After that preliminary analysis, we explicitly calculated the LO energy. As known from ref. [37], the BPS configurations that can be correctly used for that purpose must respect

JHEP11(2022)092

the (generalized) restricted harmonic condition. As shown in ref. [37], we verified again that the spherically symmetric solution of topological charge $B = 1$ respects the GRH criterion. Moreover, we also checked that the addition of the pion-mass potential to the BPS-deformation terms does not change the previous result. Apart from the topological sector $B = 1$, we have not been able to analytically find any other GRH configuration of charge $B > 1$, although we proved that in some cases their existence is necessary. Given this limitation, the only restricted-harmonic map we could build for a multi-soliton case was the one made by non-overlapping $B = 1 + 1 + 1 + \cdots$ spherical compactons.

The risk of using only the $B = 1+1+1+\cdots$ configuration as the background field is the possibility of obtaining meta-stable nuclear solutions. Other clusterization, in fact, could be energetically preferred for the nuclei built with the various near-BPS models considered here. To avoid such possibility, we analyzed the clusterization problem (at the leading-order in ϵ) by studying the ratio E/N (energy per nucleon) for the various topological sectors. Here, we denoted by $N_\star$ the most energetically favored configuration, analogously to the analysis in refs. [23, 34]. We found that a proper choice of the coefficients of the kinetic and Skyrme term ($c_4 \gg c_2 R^2$) leading to $N_\star \sim 1$, so that the single $B = 1$ Skyrmion represents the energetically favored fundamental unit of nuclei, as desired. In order to obtain physically stable nuclei given the mathematical results derived by the restricted harmonic analysis, we worked coherently in that limit.

At the leading-order in the ϵ-expansion there is no binding energy, since the BPS solution only enjoys compact support (i.e. it is a compacton). A further step in the perturbative approximation was therefore needed.

The higher-order-in-ϵ, i.e. the NLO and N^{2}LO corrections to the mass are computed in the ϵ-expansion scheme by using a linearized fluctuation field possessing three components, denoted δf, $\delta\theta$ and $\delta\varphi$. For a single $B = 1$ Skyrmion, only spherically symmetric fluctuations are turned on and only the δf field, since it is the only sourced fluctuation. In order to capture the correct behavior of the fluctuations, a special cusp condition on the boundary of the compacton must be imposed making the total field smooth at said boundary. For a single $B = 1$ Skyrmion we were able to test the predictions of the ϵ-expansion with the full numerical computation. We finally computed the binding energy of the two $B = 1$ Skyrmions bound state, corresponding to the classical version of the deuteron in the near-BPS limit in our specific model. The binding energy is maximal when the two compactons are touching each other at one point and nonspherical behavior of δf near the gluing boundary turns on the fluctuation fields $\delta\theta$ and $\delta\varphi$. Although we have not been able to test the accuracy of the binding energy of the bound state by also performing full brute-force numerical computations, we rely on the fact that the ϵ-expansion scheme is accurate for the $B = 1$ spherically symmetric soliton and that the analogous 2-dimensional analysis for the baby Skyrme model compares rather successful to full numerical computations [23].

The classical binding energy of the deuteron bound state comes out about a factor of 3 too small, but the model is quite constrained by the necessary conditions making the ϵ-expansion reliable. Moreover, the various choices that finally select the specific near-BPS model are not only made for phenomenological reasons but also for having the possibility of obtaining a mathematically consistent perturbative expansion in ϵ. In fact, to that end,

JHEP11(2022)092

we have firstly chosen BPS compacton-type solutions to simplify the restricted harmonic problem. Then, we selected among the remaining near-BPS models the ones that admit finite-energy contribution at every order in the ϵ-expansion. In the end, we dealt with the generalized restricted harmonic problem that pushed us to constrain the BPS-deformation's coefficients to obtain stable nuclei. It is therefore clear that there is no reason *a priori* to think that those constraints get the model close to the one that nature has chosen. An important question is, for example, whether the most phenomenologically viable near-BPS Skyrme model contains compactons or solitons with tails in the BPS limit that nature has chosen to be close to.

Nevertheless, this work has shown that the near-BPS model is able to reproduce the small binding energy for the deuteron (and in principle for larger nuclei) of the order of the experimental values. The near-BPS model can therefore be confirmed to be a reasonable candidate to fix the binding energy problem of the original Skyrme model and thus to be a reliable nuclear model. Moreover, the exploration of the near-BPS limit made in this work clarifies the difficulties, and thus the solutions, for a more extensive analysis of this and related models.

In light of our new understanding of the near-BPS Skyrme problem, we can reconsider the study in ref. [31]. In that work, a BPS model with the potential $(s, p) = (1, 2)$ slightly deformed by just the two-derivative kinetic term was considered. Such a deformation was coupled to the usual small parameter $\epsilon \ll 1$. Using numerical methods, the full equations of motions of the system were solved for the cases $1 \leq B \leq 8$ for the range $\epsilon \in [0.2, 1]$. On the contrary, for smaller values of ϵ ($\epsilon < 0.2$), all the results were numerically inaccessible (except for the $B = 2$ case, where axial symmetry was assumed by Ansatz). In that range, indeed, the numerical solutions develop spike-like singularities, indicating that the lattice cannot resolve the field gradients. Despite these difficulties, the work gave interesting results. First of all, the numerical simulations showed that the near-BPS solutions for a small value of $\epsilon \sim 0.2$ have different geometric symmetries (see figure 2 of ref. [31]).

This numerical outcome gives therefore (partial) confirmation of the fact that a spherical configuration is far from being a good approximation to a near-BPS solution at small ϵ for $B > 1$. This is not in contradiction with our claim. We worked in fact with specific values of potentials and couplings such that $N_\star \simeq 1$ so that a $B = 1 + 1 + 1 + \cdots$ configuration as a background field is the most reasonable candidate BPS background. For the specific case considered in ref. [31] $N_\star = 2.197$. It so happens that by the parameter choices made in our work, the values of ϵ needed are about an order of magnitude larger than those needed for the simplistic model of ref. [31], which is not inconsistent because the two models are fundamentally different.

In particular, we underline the crucial role of the generalized-restricted-harmonic study to extend the perturbative method explored here to a larger set of near-BPS models. An interesting future direction would be to consider non-spherically symmetric restricted harmonic solutions as the background BPS solutions for the near-BPS physics. So far none are known, but our results suggest that there are undiscovered solutions.

JHEP11(2022)092

Acknowledgments

S. B. G. thanks the Outstanding Talent Program of Henan University and the Ministry of Education of Henan Province for partial support. The work of S. B. G. is supported by the National Natural Science Foundation of China (Grants No. 11675223 and No. 12071111) and by the Ministry of Science and Technology of China (Grant No. G2022026021L). The work of M. B. and S. B. is supported by the INFN special project grant "GAST (Gauge and String Theories)".

A Bound on the energy

In this appendix, we will review the lower bound on the energy of the generalized Skyrme model of ref. [52] (see also ref. [27]). The general idea of the calculation utilizes the fact that the generalized Skyrme model is the sum of different subsectors, each of which has a known energy bound. Then to find the total energy bound, an optimization between the different bounds should be carried out.

Given the Lagrangian (2.1), which corresponds to the static energy (2.14), we can write

$$E = \mu^2 E_0 + \epsilon c_2 E_2 + \epsilon c_4 E_4 + c_6 E_6, \tag{A.1}$$

where E_2, E_4, and E_6 are defined in eqs. (2.16), (2.17) and (2.15), respectively and where we have defined

$$E_0 = \int_{\mathbb{R}^3} \widetilde{V}(U)\, \mathrm{d}^3x = \int_{\mathbb{R}^3} \left[V_{s,p}(U) + \frac{\epsilon m_\pi^2}{\mu^2} V_{1,1}(U) \right] \mathrm{d}^3x. \tag{A.2}$$

Then, given the energy bounds:

$$\beta E_0 + E_6 \geq 4\pi^2 \beta^{\frac{1}{2}} \langle \widetilde{V}^{\frac{1}{2}} \rangle\, |B|, \tag{A.3}$$

$$\beta E_0 + E_4 \geq 4\pi^2 (2\beta)^{\frac{1}{4}} \langle \widetilde{V}^{\frac{1}{4}} \rangle\, |B|, \tag{A.4}$$

$$\beta E_2 + E_4 \geq 6\pi^2 \beta^{\frac{1}{2}}\, |B|, \tag{A.5}$$

$$\beta E_2 + E_6 \geq 8\pi^2 \left(\frac{\beta}{2}\right)^{\frac{3}{4}} |B|\ , \tag{A.6}$$

in which we have defined $\langle \cdots \rangle$ as the target-space average of a generic quantity X as

$$\langle X \rangle \equiv -\frac{1}{24\pi^2 B} \int_{\mathbb{R}^3} X \epsilon_{ijk}\, \mathrm{tr}[L_i L_j L_k]\, \mathrm{d}^3x, \tag{A.7}$$

it is possible to rewrite the energy (A.1) as a sum of the above subsectors introducing four parameters α_{2i} with $0 \leq \alpha_{2i} \leq 1$ for $i = 0, \ldots, 3$, that determine how each term is split between the given bounds. The general bound for the total energy as a function of $\{\alpha_i\}$ is

JHEP11(2022)092

thus:

$$
\begin{aligned}
E &= (\alpha_0\mu^2 E_0 + \alpha_6 c_6 E_6) + ((1-\alpha_0)\mu^2 E_0 + \alpha_4 \epsilon c_4 E_4) \\
&\quad + (\alpha_2 \epsilon c_2 E_2 + (1-\alpha_4)\epsilon c_4 E_4) + ((1-\alpha_2)\epsilon c_2 E_2 + (1-\alpha_6) c_6 E_6) \\
&\geq 2\pi^2 \Bigg[2\mu (\alpha_0 \alpha_6 c_6)^{\frac{1}{2}} \langle \widetilde{V}^{\frac{1}{2}} \rangle + 2\sqrt{\mu} (\alpha_4 \epsilon c_4)^{\frac{3}{4}} \big(2(1-\alpha_0)\big)^{\frac{1}{4}} \langle \widetilde{V}^{\frac{1}{4}} \rangle \\
&\qquad + 3\epsilon \big((1-\alpha_4) c_4 \alpha_2 c_2\big)^{\frac{1}{2}} + 4\big((1-\alpha_6) c_6\big)^{\frac{1}{4}} \left(\frac{1}{2}(1-\alpha_2)\epsilon c_2 \right)^{\frac{3}{4}} \Bigg] |B|. \qquad \text{(A.8)}
\end{aligned}
$$

Once we have chosen the potential $\widetilde{V}(U)$ and the parameters c_0, c_2, c_4 and c_6, the strongest energy bound for the system is the maximum of the functional (A.8), which is a maximization problem in four variables (α_i). It is difficult to write down an analytic solution to the solution of the maximization problem, but it is rather easy to find numerically.

References

[1] T.H.R. Skyrme, *A Nonlinear field theory*, *Proc. Roy. Soc. Lond. A* **260** (1961) 127 [INSPIRE].

[2] T.H.R. Skyrme, *A Unified Field Theory of Mesons and Baryons*, *Nucl. Phys.* **31** (1962) 556 [INSPIRE].

[3] E. Witten, *Global Aspects of Current Algebra*, *Nucl. Phys. B* **223** (1983) 422 [INSPIRE].

[4] E. Witten, *Current Algebra, Baryons, and Quark Confinement*, *Nucl. Phys. B* **223** (1983) 433 [INSPIRE].

[5] E. Witten, *Anti-de Sitter space, thermal phase transition, and confinement in gauge theories*, *Adv. Theor. Math. Phys.* **2** (1998) 505 [hep-th/9803131] [INSPIRE].

[6] T. Sakai and S. Sugimoto, *Low energy hadron physics in holographic QCD*, *Prog. Theor. Phys.* **113** (2005) 843 [hep-th/0412141] [INSPIRE].

[7] G.S. Adkins, C.R. Nappi and E. Witten, *Static Properties of Nucleons in the Skyrme Model*, *Nucl. Phys. B* **228** (1983) 552 [INSPIRE].

[8] C.J. Halcrow, *Vibrational quantisation of the $B = 7$ Skyrmion*, *Nucl. Phys. B* **904** (2016) 106 [arXiv:1511.00682] [INSPIRE].

[9] S. Bjarke Gudnason and C. Halcrow, *Vibrational modes of Skyrmions*, *Phys. Rev. D* **98** (2018) 125010 [arXiv:1811.00562] [INSPIRE].

[10] S.B. Gudnason and C. Halcrow, *A SMörgåsbord of Skyrmions*, *JHEP* **08** (2022) 117 [arXiv:2202.01792] [INSPIRE].

[11] B. Zumino, *Supersymmetry and Kähler Manifolds*, *Phys. Lett. B* **87** (1979) 203 [INSPIRE].

[12] E.A. Bergshoeff, R.I. Nepomechie and H.J. Schnitzer, *Supersymmetric Skyrmions in Four-dimensions*, *Nucl. Phys. B* **249** (1985) 93 [INSPIRE].

JHEP11(2022)092

[13] A.A. Bogolubskaya and I.L. Bogolubsky, *Stationary Topological Solitons in the Two-dimensional Anisotropic Heisenberg Model With a Skyrme Term*, *Phys. Lett. A* **136** (1989) 485 [INSPIRE].

[14] A.A. Bogolyubskaya and I.L. Bogolyubsky, *On stationary topological solitons in two-dimensional anisotropic Heisenberg model*, *Lett. Math. Phys.* **19** (1990) 171 [INSPIRE].

[15] B.M.A.G. Piette, B.J. Schroers and W.J. Zakrzewski, *Multi - solitons in a two-dimensional Skyrme model*, *Z. Phys. C* **65** (1995) 165 [hep-th/9406160] [INSPIRE].

[16] C. Adam, J.M. Queiruga, J. Sanchez-Guillen and A. Wereszczynski, $N = 1$ *supersymmetric extension of the baby Skyrme model*, *Phys. Rev. D* **84** (2011) 025008 [arXiv:1105.1168] [INSPIRE].

[17] S. Bolognesi and W. Zakrzewski, *Baby Skyrme Model, Near-BPS Approximations and Supersymmetric Extensions*, *Phys. Rev. D* **91** (2015) 045034 [arXiv:1407.3140] [INSPIRE].

[18] C. Adam, J.M. Queiruga, J. Sanchez-Guillen and A. Wereszczynski, *Extended Supersymmetry and BPS solutions in baby Skyrme models*, *JHEP* **05** (2013) 108 [arXiv:1304.0774] [INSPIRE].

[19] M. Nitta and S. Sasaki, *BPS States in Supersymmetric Chiral Models with Higher Derivative Terms*, *Phys. Rev. D* **90** (2014) 105001 [arXiv:1406.7647] [INSPIRE].

[20] M. Nitta and S. Sasaki, *Classifying BPS States in Supersymmetric Gauge Theories Coupled to Higher Derivative Chiral Models*, *Phys. Rev. D* **91** (2015) 125025 [arXiv:1504.08123] [INSPIRE].

[21] S.B. Gudnason, M. Nitta and S. Sasaki, *A supersymmetric Skyrme model*, *JHEP* **02** (2016) 074 [arXiv:1512.07557] [INSPIRE].

[22] S.B. Gudnason, M. Nitta and S. Sasaki, *Topological solitons in the supersymmetric Skyrme model*, *JHEP* **01** (2017) 014 [arXiv:1608.03526] [INSPIRE].

[23] S.B. Gudnason, M. Barsanti and S. Bolognesi, *Near-BPS baby Skyrmions*, *JHEP* **11** (2020) 062 [arXiv:2006.01726] [INSPIRE].

[24] P. Sutcliffe, *Skyrmions, instantons and holography*, *JHEP* **08** (2010) 019 [arXiv:1003.0023] [INSPIRE].

[25] C. Adam, J. Sanchez-Guillen and A. Wereszczynski, *A Skyrme-type proposal for baryonic matter*, *Phys. Lett. B* **691** (2010) 105 [arXiv:1001.4544] [INSPIRE].

[26] C. Adam, J. Sanchez-Guillen and A. Wereszczynski, *A BPS Skyrme model and baryons at large N_c*, *Phys. Rev. D* **82** (2010) 085015 [arXiv:1007.1567] [INSPIRE].

[27] D. Harland, *Topological energy bounds for the Skyrme and Faddeev models with massive pions*, *Phys. Lett. B* **728** (2014) 518 [arXiv:1311.2403] [INSPIRE].

[28] C. Adam, K. Oles and A. Wereszczynski, *The Dielectric Skyrme model*, *Phys. Lett. B* **807** (2020) 135560 [arXiv:2005.00018] [INSPIRE].

[29] P. Sutcliffe, *Skyrmions in a truncated BPS theory*, *JHEP* **04** (2011) 045 [arXiv:1101.2402] [INSPIRE].

[30] C. Naya and P. Sutcliffe, *Skyrmions in models with pions and rho mesons*, *JHEP* **05** (2018) 174 [arXiv:1803.06098] [INSPIRE].

[31] M. Gillard, D. Harland and M. Speight, *Skyrmions with low binding energies*, *Nucl. Phys. B* **895** (2015) 272 [arXiv:1501.05455] [INSPIRE].

JHEP11(2022)092

[32] N.S. Manton and P. Sutcliffe, *Topological solitons*, Cambridge Monographs on Mathematical Physics, Cambridge University Press (2004), 10.1017/CBO9780511617034 [INSPIRE].

[33] S.B. Gudnason, *Dielectric Skyrmions*, *Phys. Rev. D* **102** (2020) 116013 [arXiv:2009.03082] [INSPIRE].

[34] S.B. Gudnason, M. Barsanti and S. Bolognesi, *Near-BPS baby Skyrmions with Gaussian tails*, *JHEP* **05** (2021) 134 [arXiv:2102.12134] [INSPIRE].

[35] E. Bonenfant and L. Marleau, *Nuclei as near BPS-Skyrmions*, *Phys. Rev. D* **82** (2010) 054023 [arXiv:1007.1396] [INSPIRE].

[36] E. Bonenfant, L. Harbour and L. Marleau, *Near-BPS Skyrmions: Non-shell configurations and Coulomb effects*, *Phys. Rev. D* **85** (2012) 114045 [arXiv:1205.1414] [INSPIRE].

[37] J.M. Speight, *Near BPS Skyrmions and Restricted Harmonic Maps*, *J. Geom. Phys.* **92** (2015) 30 [arXiv:1406.0739] [INSPIRE].

[38] R. Battye and P. Sutcliffe, *Skyrmions and the pion mass*, *Nucl. Phys. B* **705** (2005) 384 [hep-ph/0410157] [INSPIRE].

[39] R. Battye and P. Sutcliffe, *Skyrmions with massive pions*, *Phys. Rev. C* **73** (2006) 055205 [hep-th/0602220] [INSPIRE].

[40] S.B. Gudnason and M. Nitta, *Fractional Skyrmions and their molecules*, *Phys. Rev. D* **91** (2015) 085040 [arXiv:1502.06596] [INSPIRE].

[41] S.B. Gudnason and M. Nitta, *A higher-order Skyrme model*, *JHEP* **09** (2017) 028 [arXiv:1705.03438] [INSPIRE].

[42] B.J. Schroers, *Dynamics of moving and spinning Skyrmions*, *Z. Phys. C* **61** (1994) 479 [hep-ph/9308236] [INSPIRE].

[43] S.B. Gudnason and J.M. Speight, *Realistic classical binding energies in the ω-Skyrme model*, *JHEP* **07** (2020) 184 [arXiv:2004.12862] [INSPIRE].

[44] G.L. Greene, E.G. Kessler, R.D. Deslattes and H. Boerner, *New Determination of the Deuteron Binding Energy and the Neutron Mass*, *Phys. Rev. Lett.* **56** (1986) 819 [INSPIRE].

[45] V.B. Kopeliovich and B.E. Stern, *Exotic Skyrmions*, *JETP Lett.* **45** (1987) 203 [INSPIRE].

[46] N.S. Manton, *Is the $B = 2$ Skyrmion Axially Symmetric?*, *Phys. Lett. B* **192** (1987) 177 [INSPIRE].

[47] J.J.M. Verbaarschot, *Axial Symmetry of Bound Baryon Number Two Solution of the Skyrme Model*, *Phys. Lett. B* **195** (1987) 235 [INSPIRE].

[48] S.B. Gudnason and M. Nitta, *Modifying the pion mass in the loosely bound Skyrme model*, *Phys. Rev. D* **94** (2016) 065018 [arXiv:1606.02981] [INSPIRE].

[49] S.B. Gudnason, B. Zhang and N. Ma, *Generalized Skyrme model with the loosely bound potential*, *Phys. Rev. D* **94** (2016) 125004 [arXiv:1609.01591] [INSPIRE].

[50] S.B. Gudnason, *Exploring the generalized loosely bound Skyrme model*, *Phys. Rev. D* **98** (2018) 096018 [arXiv:1805.10898] [INSPIRE].

[51] Flavour Lattice Averaging Group (FLAG) collaboration, *FLAG Review 2021*, *Eur. Phys. J. C* **82** (2022) 869 [arXiv:2111.09849] [INSPIRE].

[52] C. Adam and A. Wereszczynski, *Topological energy bounds in generalized Skyrme models*, *Phys. Rev. D* **89** (2014) 065010 [arXiv:1311.2939] [INSPIRE].

JHEP11(2022)092